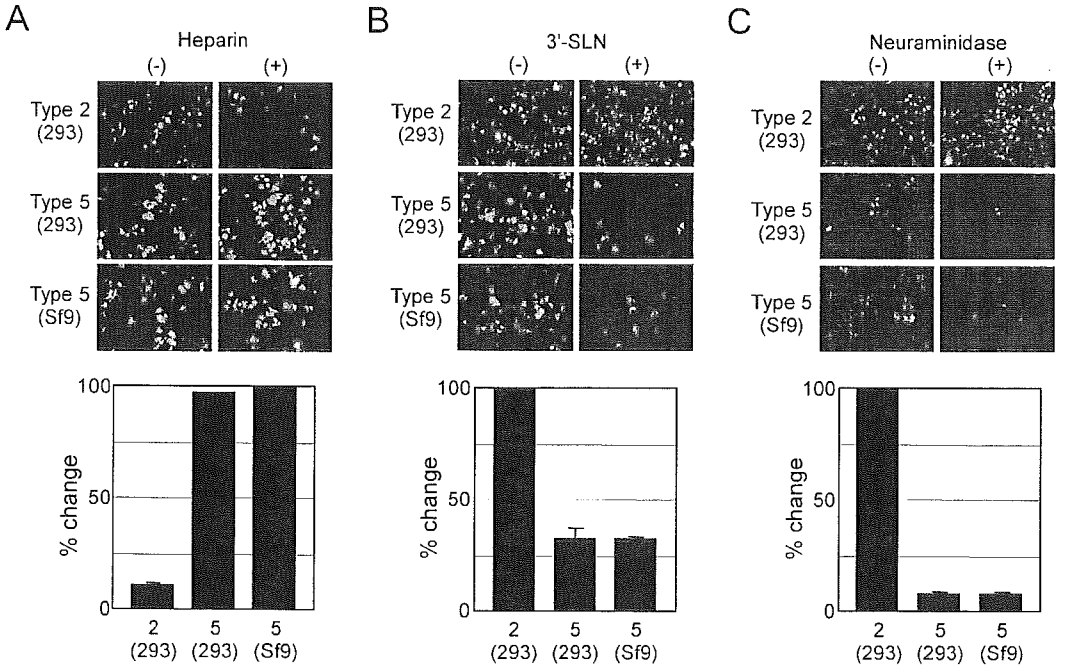

FIG. 6. (A) Heparin, an analog of HSPG, does not inhibit transduction of COS cells infected with rAAV5-GFP/Neo produced in insect cells. Cells were infected with adenovirus at 3 PFU per cell and incubated at 37°C for 2 h. After being washed with medium, the cells were infected with rAAV2-GFP/Neo produced in 293 cells at 10^4 vg per cell or rAAV5-GFP/Neo generated in 293 cells or Sf9 cells at 10^5 vg per cell in the presence or absence of 20 μg per ml of heparin in triplicate. One day after infection, the cells were observed under a fluorescent microscope. The number of GFP-positive cells was also counted by flow cytometry. Data are presented as percent change in transduction compared to transduction in the absence of heparin. (B) An analog of α2-3 sialic acid inhibits both 293 cell- and Sf9 cell-produced rAAV5-GFP/Neo. COS cells were infected with an adenovirus at 3 PFU per cell and incubated at 37°C for 2 h. After being washed with medium, the cells were infected with rAAV2-GFP/Neo at 10^4 vg per cell or rAAV5-GFP at 10^5 vg per cell for 1.5 h in the presence of 0 or 0.5 mM 3′-SLN (Sigma-Aldrich). The cells were washed twice with medium and further incubated for 1 day. The number of GFP-expressing cells was measured by flow cytometry ($n = 3$). Data are presented as percent change in transduction compared to transduction in the absence of the analog. (C) Neuraminidase treatment of COS cells inhibits transduction with rAAV5-GFP generated in 293 cells or Sf9 cells. COS cells were infected in triplicate with adenovirus at 3 PFU per cell for 1 h at 37°C, treated with 0.08 U per ml of neuraminidase (*Vibrio cholerae*, type III; Sigma-Aldrich) for 1 h, and infected with 10^5 vg per cell of rAAV5-GFP produced in 293 cells or Sf9 cells for 2 h. COS cells were similarly treated and also infected with 10^4 vg per cell of rAAV2-GFP/Neo. The infected cells were then washed twice with medium and incubated for an additional day. After incubation, the cells were observed under fluorescent microscopy and the number of GFP-positive cells was counted by flow cytometry.

two DNA species. The higher-mobility virion DNA corresponds with 2.4-kb hGFP vector DNA or a single-stranded monomer, which is confirmed by comigration with a 2.4-kb vector DNA obtained by treatment with a restriction enzyme of the hGFP vector plasmid, pSR485hGFP. The lower-mobility DNA is the same in size as the monomer RF or duplex form of hGFP DNA (Fig. 7D) isolated from Sf9 cells coinfected with RepBac and hGFPBac (Fig. 4C). The intensity of the larger virion DNA, which was quantified with an imaging analyzer, was roughly double that of shorter DNA for each rAAV5 produced in Sf9 cells. If the larger virion DNA is a monomer duplex form and thus has two CMV promoter sequences hybridizing to a CMV probe, then we estimated that the quantity of the double-stranded monomeric form was equal to that of the single-stranded monomer. The ratio of the amount of the monomer duplex form to the amount of the single-stranded monomer form in the rAAV5-hGFP virion produced in 293 cells is 1 to 3.5. AAV particles have been shown to package two copies of vector genomes that are less than 50% of the 4.8-kb AAV genome, and the packaged vector DNA appeared to be monomeric single-stranded and double-stranded RF (6). For gene expression, the single-stranded vector genome has to be converted to a double-stranded form by either second-strand synthesis (8, 9) or annealing of complementary strands (23). The monomeric duplex vector DNA, on the other hand, can function directly as a template for mRNA synthesis. Thus, the more potent gene expression mediated by rAAV5-hGFP generated in Sf9 cells is probably due to the presence of the encapsidated monomer duplex form.

Comparison of efficacies of rAAV5 in vivo. To compare the efficacies of rAAV5 produced in 293 cells and rAAV5 produced in Sf9 cells, we constructed a type 5 vector that expressed human SEAP. rAAV5 particles produced in Sf9 cells consisted of chimeric VP1 between type 2 and type 5. To eliminate the possible difference in intracellular processing of rAAV5 particles due to replacement of the type 5 VP1-unique portion with the equivalent one of type 2, we compared the in vivo activities of rAAV5 particles containing type 2/5 VP1 polypeptides produced in insect and mammalian cells. Five mice each intramuscularly received a total of 10^{11} vg of rAAV5-SEAP generated in either 293 cells or Sf9 cells, and serum SEAP levels were monitored. As shown in Fig. 8A, the expression profile of the Sf9-produced type 5 SEAP vector differed from that of the 293-produced one. The rAAV5-SEAP

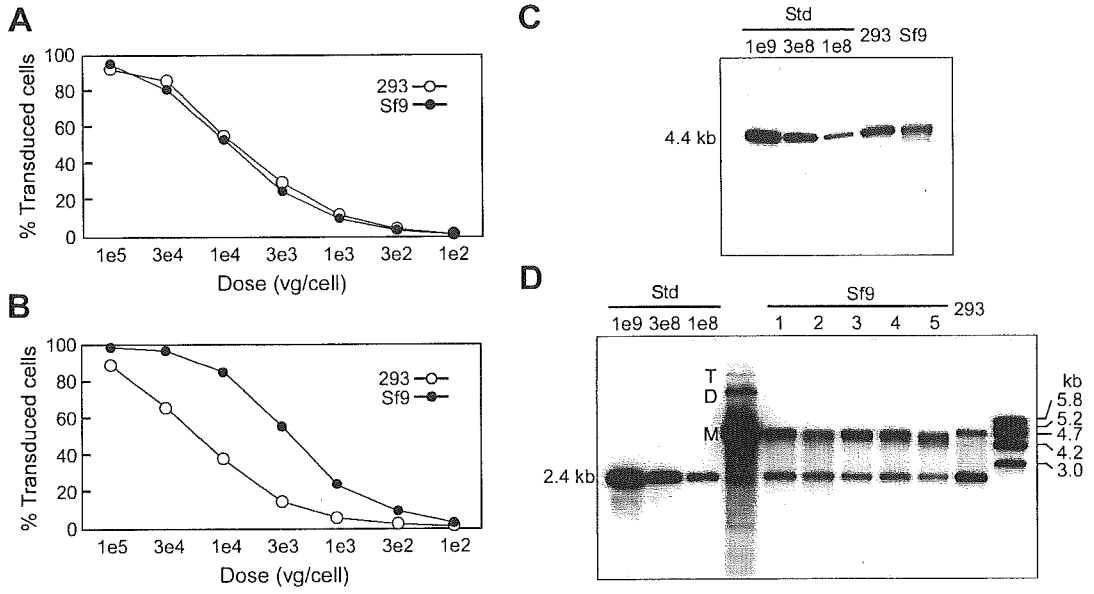

FIG. 7. Comparison of infectivities of rAAV5 produced in 293 cells and rAAV5 produced in Sf9 cells. (A) COS cells were infected with rAAV5-GFP/Neo produced in 293 cells or Sf9 cells at the doses indicated, ranging from 1×10^5 through 1×10^2 vg per cell. One day after infection, the cells were examined for GFP fluorescence by flow cytometry in triplicate. (B) COS cells were infected with rAAV5-hGFP produced in HEK293 cells or Sf9 cells at a dose of 1×10^5 through 1×10^2 vg per cell for 1 day. The number of GFP-positive cells was counted cytometrically. (C) Analysis of GFP/Neo vector virion DNA on an alkaline gel. Virion DNA was isolated from rAAV5-GFP/Neo produced in HEK293 cells or Sf9 cells by treatment with proteinase K, and samples equivalent to 3×10^8 vg were resolved onto a 0.8% alkaline gel. The DNA was then transferred to a nylon membrane and hybridized to a ^{32}P-labeled CMV-specific probe. A 4.4-kb-size copy number standard (Std) (1×10^9, 3×10^8, and 1×10^8 copies) was loaded, which was derived from the GFP/Neo vector plasmid, pSR485α, with a restriction enzyme that cut out the vector portion. (D) Alkaline agarose gel electrophoresis of virion DNA isolated from rAAV5-hGFP. Vector DNA isolated from rAAV5-hGFP particles produced with type 1, 2, 3, 4, or 5 Rep52 was analyzed along with 293-produced rAAV5-hGFP. Low-molecular-weight DNA isolated from insect cells infected with RepBac and hGFPBac (Fig. 4C) serves as a reference for monomer (M), dimer (D), and trimer (T) replicative forms.

generated in HEK293 cells showed a gradual increase in serum SEAP activity over 1 month after injection, which is a typical expression pattern by rAAV-mediated transduction. The Sf9-produced rAAV5-SEAP induced levels of SEAP activity at 1 or 2 weeks after injection that were more than 30 or 10 times higher, respectively, than those of the 293-produced rAAV5-SEAP, and the serum SEAP activity by Sf9 produced rAAV5-SEAP decreased at 4 weeks after injection. There was no significant difference between the two groups after 4 weeks following administration. We also analyzed the SEAP vector DNA on an alkaline gel (Fig. 8B). The expected size of rAAV5-SEAP vector genomes is 3.4 kb. The majority of 293-produced rAAV5-SEAP DNA is single-stranded monomer in both type 5 capsids and type 2/5 chimeric capsids. In addition to the 3.4-kb single-stranded vector genome, DNA extracted from Sf9 cell-produced rAAV5 particles contained an additional DNA of approximately 4.7 kb. One model for AAV packaging proposes that when the size of vector DNA is larger than the size of the wild-type AAV, 4.7 kb, the vector DNA is cleaved to 100% of the AAV genome during packaging into virion (6). The 4.7-kb virion DNA may be a cleaved product of duplex multimers synthesized in Sf9 cells.

DISCUSSION

Recent advances in understanding of biology of AAV and in production of rAAV have facilitated the use of rAAV as a gene transfer vector. A human clinical trial with rAAV2 expressing a coagulation factor IX has shown that intramuscular delivery of more than 10^{15} rAAV2 particles would be required for amelioration of hemophilia B (15). Currently, the widely employed method for production of rAAV is transfection of packaging cells, such as HEK293 cells, with plasmids carrying AAV and adenovirus genes. Plasmid transfection is more easily adaptable to packaging different serotype AAV vectors than establishing a packaging cell line. However, the transfection process is the limiting step in rAAV production, which requires adherent HEK293 cells on a two-dimensional surface for efficient production of rAAV.

The production of other AAV serotype-derived vectors has been described previously (26) and follows the strategy developed for rAAV2 (20). Some modifications have been reported, such as lipofection of 293 cells in suspension culture in serum-free media, which makes the handling of the cells and the purification step easier (28). However, the use of a lipid reagent for transfection may be neither cost-effective nor scalable. A recombinant herpes simplex virus harboring type 5 *rep* and *cap* genes was created to eliminate the transfection process (33), although the yields of rAAV5 were low. The baculovirus/insect cell-based rAAV5 production system presented here does not require plasmid transfection and is scalable. By extrapolation from culture volume, we expect to obtain more than 10^{14} particles of rAAV5-GFP from a 1-liter culture. This is consistent with yields of rAAV1 or rAAV2 produced in Sf9 cell cultures (20a, 31).

To produce infectious rAAV5 particles in insect cells, we

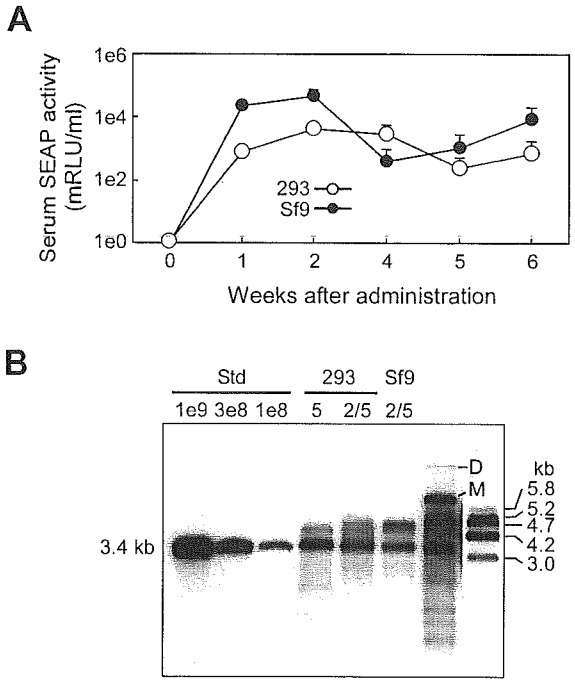

FIG. 8. (A) Serum SEAP activity following intramuscular injection of rAAV5-SEAP. Five mice each received a total of 10^{11} vg of pseudotyped rAAV5-SEAP produced in 293 cells or Sf9 cells into tibialis anterior muscles. Blood was taken at the indicated weeks after injection. The serum SEAP activity was measured by a SEAP report gene assay (Roche Diagnostics, GmbH, Penzberg, Germany). RLU, relative light units. (B) Molecular analysis of SEAP vector DNA. Vector genomes were isolated from type 5 or type 2/5 SEAP vector particles produced in HEK293 cells or from Sf9-produced rAAV5-SEAP. Extrachromosomal low-molecular-weight DNA isolated from Sf9 cells infected with RepBac and SEAPBac was also analyzed. Copies (10^9 through 10^8) of copy number standard (Std) vector DNA derived from SEAP vector plasmid, pAAVSEAP, were also loaded. M, monomer replicative form of SEAP vector genomes; D, dimer replicative form.

inserted an N-terminal portion of type 2 VP1 into the corresponding site of type 5 VP1. The N termini of VP1 polypeptides contain the phospholipase A_2 motif and are essential to viral infectivity (36). Electron microscopy indicated that the VP1-unique portion is hidden within type 2 capsids and appears on the surface of the capsids during the infectious pathway in cells (19). The VP1-unique portion is well conserved among different AAVs. Comparison of the portion among serotypes 1 through 4 and 6 revealed that one serotype is more than 80% identical to another. The type 5 VP1-unique portion is 70 to 75% identical to that of other serotypes, while the sequence alignment of VP2 or VP3 of AAV1 through AAV6 showed that type 5 is approximately 55% identical to other serotypes. The initial trial mutation of the start codon for type 5 VP1 gene to ACG failed to produce infectious rAAV5 particles due to low synthesis of VP1 polypeptide (Fig. 2C). However, the successful generation of rAAV2 particles in insect cells and the notion that the VP1-specific region is well conserved among different serotypes led us to construct a chimeric type 5 VP1 polypeptide whose N-terminal portion was partially replaced by the equivalent portion of type 2. The transduction of COS cells and mouse muscles with rAAV5 produced in insect cells clearly indicated that the chimeric VP1, VP254, could confer infectivity to it (Fig. 7 and 8).

The strategy of producing AAV "pseudotyped" vectors, typically consisting of AAV2 ITR and non-AAV2 capsids, such as AAV4 and AAV5, has been reported previously (2, 3, 26, 34). We first tested similar pseudopackaging of rAAV DNA type 2 ITRs into type 5 capsids with type 2 RepBac in insect cells. However, the yields of vector particles produced were four times lower than those reached by packaging type 5 DNA into type 5 capsids (data not shown). We also examined the production of rAAV5 by packaging type 2 AAV DNA with type 2 Rep78 and type 5 Rep52 into type 5 capsids, which also resulted in low yields of rAAV5 (data not shown). The production of type 5 vector in 293 cells by transfection with a type 5 vector plasmid and a type 5 *rep cap* plasmid usually yields more than 10^4 particles per HEK293 cell, and the production of pseudotyped type 5 vectors by using a type 2 AAV vector plasmid and type 2 *rep* and type 5 *cap* plasmid recovers 3×10^3 particles per cell (unpublished observation), an observation consistent with the production in Sf9 cells.

Using Sf9 cells, we found that Rep52 proteins of other serotypes were capable of packaging DNA with type 5 ITRs into type 5 capsids more efficiently than type 5 Rep52. Type 2 small Rep protein has been shown to package the AAV2 genome into preformed capsid with its helicase activity in collaboration with large Rep protein (7, 17). The small Rep protein associates with Rep78/68 (24) and probably specifically interacts with large Rep protein during encapsidation (7). The basis for the improved AAV packaging with non-type 5 Rep52 remains to be elucidated. To exclude the possibility that cellular proteins and/or baculovirus proteins played a major role in packaging type 5 DNA, we used a RepBac that expressed only type 5 Rep78 for production of type 5 rAAV. No rAAV5 particles were recovered from the recombinant baculovirus-infected Sf9 cells (data not shown), suggesting that the small Rep protein is absolutely required for generating rAAV5 in insect cells. As shown in Fig. 5F, the fact that the partial replacement of the VP1-unique portion with the corresponding portion of type 2, the strategy we took to generate infectious type 5 particles in insect cells, inhibited type 5 Rep52-mediated introduction of type 5 ITR genomes into type 5 capsids may only indicate the role of the type 2 VP1-unique portion as a physical barrier during packaging of rAAV genomes into capsids. We believe that under a special circumstance, such as in invertebrate cells, heteroserotypic Rep52 is superior to type 5 Rep52 in packaging rAAV DNA with type 5 ITR into type 5 capsids. It is interesting to examine whether other serotypes of Rep52 can package type 5 rAAV DNA into type 5 capsid in mammalian cells. We are currently investigating the packaging of type 5 genome into type 5 capsids with different serotypes of Rep52 in HEK293 cells.

The majority of the vector genome of rAAV5 produced in HEK293 cells in the present study is in single-stranded monomeric form, irrespective of the size of the vector genome (Fig. 7C and D and 8B). However, when the size of vector DNA is shorter than the size of the wild-type AAV genome, insect cells tend to package longer, 4.7-kb DNA into type 5 capsids. The 4.7-kb longer virion DNA in Sf9-produced rAAV5 appears to be a cleavage product of multimers of replicated vector genomes. If the size of a multimer is within the packaging limit,

it is efficiently introduced into AAV capsids. If a multimer is larger than 4.8 kb in size, a partially truncated multimer is packaged into AAV capsids in insect cells (6). Sequencing of 4.7-kb DNA packaged into virions will be a key to disclosing the difference between packaging of vector DNA into capsids in HEK293 cells and insect cells. The difference in packaged virion DNA between rAAV5 produced in human cells and in insect cells provides important information on designing vector DNA for production of rAAV5 in insect cells.

In summary, we developed a new method for production of rAAV5 in insect cells, which offers a better alternative to the existing production methods of rAAV5, although the vector genomes packaged into capsids differ in size from rAAV5 produced in HEK293 cells. The robust generation in suspension culture will facilitate the use of type 5 rAAV not only for basic studies but also for clinical studies.

ACKNOWLEDGMENTS

This work was supported in part by grants from the Ministry of Health, Welfare, and Labor of Japan and Grants-in-Aid for Scientific Research from the Ministry of Education, Science, Sports, and Technology of Japan, and High-Tech Research Center Project for private universities (matching-fund subsidy from the Ministry of Education, Science, Sports, and Technology of Japan). This research was also supported in part by the Intramural Research Program of the NHLBI, NIH.

REFERENCES

1. **Balsinde, J., M. A. Balboa, P. A. Insel, and E. A. Dennis.** 1999. Regulation and inhibition of phospholipase A2. Annu. Rev. Pharmacol. Toxicol. **39:**175–189.
2. **Chiorini, J. A., F. Kim, L. Yang, and R. M. Kotin.** 1999. Cloning and characterization of adeno-associated virus type 5. J. Virol. **73:**1309–1319.
3. **Chiorini, J. A., L. Yang, Y. Liu, B. Safer, and R. M. Kotin.** 1997. Cloning of adeno-associated virus type 4 (AAV4) and generation of recombinant AAV4 particles. J. Virol. **71:**6823–6833.
4. **Conway, J. E., C. M. Rhys, I. Zolotukhin, S. Zolotukhin, N. Muzyczka, G. S. Hayward, and B. J. Byrne.** 1999. High-titer recombinant adeno-associated virus production utilizing a recombinant herpes simplex virus type I vector expressing AAV-2 Rep and Cap. Gene Ther. **6:**986–993.
5. **Davidson, B. L., C. S. Stein, J. A. Heth, I. Martins, R. M. Kotin, T. A. Derksen, J. Zabner, A. Ghodsi, and J. A. Chiorini.** 2000. Recombinant adeno-associated virus type 2, 4, and 5 vectors: transduction of variant cell types and regions in the mammalian central nervous system. Proc. Natl. Acad. Sci. USA **97:**3428–3432.
6. **Dong, J. Y., P. D. Fan, and R. A. Frizzell.** 1996. Quantitative analysis of the packaging capacity of recombinant adeno-associated virus. Hum. Gene Ther. **7:**2101–2112.
7. **Dubielzig, R., J. A. King, S. Weger, A. Kern, and J. A. Kleinschmidt.** 1999. Adeno-associated virus type 2 protein interactions: formation of pre-encapsidation complexes. J. Virol. **73:**8989–8998.
8. **Ferrari, F. K., T. Samulski, T. Shenk, and R. J. Samulski.** 1996. Second-strand synthesis is a rate-limiting step for efficient transduction by recombinant adeno-associated virus vectors. J. Virol. **70:**3227–3234.
9. **Fisher, K. J., G. P. Gao, M. D. Weitzman, R. DeMatteo, J. F. Burda, and J. M. Wilson.** 1996. Transduction with recombinant adeno-associated virus for gene therapy is limited by leading-strand synthesis. J. Virol. **70:**520–532.
10. **Gao, G. P., G. Qu, L. Z. Faust, R. K. Engdahl, W. Xiao, J. V. Hughes, P. W. Zoltick, and J. M. Wilson.** 1998. High-titer adeno-associated viral vectors from a Rep/Cap cell line and hybrid shuttle virus. Hum. Gene Ther. **9:**2353–2362.
11. **Grunert, S., and R. J. Jackson.** 1994. The immediate downstream codon strongly influences the efficiency of utilization of eukaryotic translation initiation codons. EMBO J. **13:**3618–3630.
12. **Hirt, B.** 1967. Selective extraction of polyoma DNA from infected mouse cell cultures. J. Mol. Biol. **26:**365–369.
13. **Hölscher, C., J. A. Kleinschmidt, and A. Bürkle.** 1995. High-level expression of adeno-associated virus (AAV) Rep78 or Rep68 protein is sufficient for infectious-particle formation by a *rep*-negative AAV mutant. J. Virol. **69:**6880–6885.
14. **Kaludov, N., K. E. Brown, R. W. Walters, J. Zabner, and J. A. Chiorini.** 2001. Adeno-associated virus serotype 4 (AAV4) and AAV5 both require sialic acid binding for hemagglutination and efficient transduction but differ in sialic acid linkage specificity. J. Virol. **75:**6884–6893.
15. **Kay, M. A., C. S. Manno, M. V. Ragni, P. J. Larson, L. B. Couto, A. McClelland, B. Glader, A. J. Chew, S. J. Tai, R. W. Herzog, V. Arruda, F. Johnson, C. Scallan, E. Skarsgard, A. W. Flake, and K. A. High.** 2000. Evidence for gene transfer and expression of factor IX in haemophilia B patients treated with an AAV vector. Nat. Genet. **24:**257–261.
16. **Kern, A., K. Schmidt, C. Leder, O. J. Muller, C. E. Wobus, K. Bettinger, C. W. Von der Lieth, J. A. King, and J. A. Kleinschmidt.** 2003. Identification of a heparin-binding motif on adeno-associated virus type 2 capsids. J. Virol. **77:**11072–11081.
17. **King, J. A., R. Dubielzig, D. Grimm, and J. A. Kleinschmidt.** 2001. DNA helicase-mediated packaging of adeno-associated virus type 2 genomes into preformed capsids. EMBO J. **20:**3282–3291.
18. **Kozak, M.** 1986. Point mutations define a sequence flanking the AUG initiator codon that modulates translation by eukaryotic ribosomes. Cell **44:**283–292.
19. **Kronenberg, S., B. Bottcher, C. W. von der Lieth, S. Bleker, and J. A. Kleinschmidt.** 2005. A conformational change in the adeno-associated virus type 2 capsid leads to the exposure of hidden VP1 N termini. J. Virol. **79:**5296–5303.
20. **Matsushita, T., S. Elliger, C. Elliger, G. Podsakoff, L. Villarreal, G. J. Kurtzman, Y. Iwaki, and P. Colosi.** 1998. Adeno-associated virus vectors can be efficiently produced without helper virus. Gene Ther. **5:**938–945.

20a. **Meghrous, J., M. G. Aucoin, D. Jacob, P. S. Chahal, N. Arcand, and A. A. Kamen.** 2005. Production of recombinant adeno-associated viral vectors using a baculovirus/insect cell suspension culture system: from shake flasks to a 20-L bioreactor. Biotechol. Prog. **21:**154–160.

21. **Murakami, M., and I. Kudo.** 2004. Secretory phospholipase A2. Biol. Pharm. Bull. **27:**1158–1164.
22. **Muramatsu, S., H. Mizukami, N. S. Young, and K. E. Brown.** 1996. Nucleotide sequencing and generation of an infectious clone of adeno-associated virus 3. Virology **221:**208–217.
23. **Nakai, H., T. A. Storm, and M. A. Kay.** 2000. Recruitment of single-stranded recombinant adeno-associated virus vector genomes and intermolecular recombination are responsible for stable transduction of liver in vivo. J. Virol. **74:**9451–9463.
24. **Pereira, D. J., D. M. McCarty, and N. Muzyczka.** 1997. The adeno-associated virus (AAV) Rep protein acts as both a repressor and an activator to regulate AAV transcription during a productive infection. J. Virol. **71:**1079–1088.
25. **Qiu, J., R. Nayak, G. E. Tullis, and D. J. Pintel.** 2002. Characterization of the transcription profile of adeno-associated virus type 5 reveals a number of unique features compared to previously characterized adeno-associated viruses. J. Virol. **76:**12435–12447.
26. **Rabinowitz, J. E., F. Rolling, C. Li, H. Conrath, W. Xiao, X. Xiao, and R. J. Samulski.** 2002. Cross-packaging of a single adeno-associated virus (AAV) type 2 vector genome into multiple AAV serotypes enables transduction with broad specificity. J. Virol. **76:**791–801.
27. **Smith, R. H., S. A. Afione, and R. M. Kotin.** 2002. Transposase-mediated construction of an integrated adeno-associated virus type 5 helper plasmid. BioTechniques **33:**204–206, 208, 210–211.
28. **Smith, R. H., C. Ding, and R. M. Kotin.** 2003. Serum-free production and column purification of adeno-associated virus type 5. J. Virol. Methods **114:**115–124.
29. **Snyder, R. O.** 1999. Adeno-associated virus-mediated gene delivery. J. Gene Med. **1:**166–175.
30. **Summerford, C., and R. J. Samulski.** 1998. Membrane-associated heparan sulfate proteoglycan is a receptor for adeno-associated virus type 2 virions. J. Virol. **72:**1438–1445.
31. **Urabe, M., C. Ding, and R. M. Kotin.** 2002. Insect cells as a factory to produce adeno-associated virus type 2 vectors. Hum. Gene Ther. **13:**1935–1943.
32. **Weyer, U., and R. D. Possee.** 1989. Analysis of the promoter of the Autographa californica nuclear polyhedrosis virus p10 gene. J. Gen. Virol. **70:**203–208.
33. **Wustner, J. T., S. Arnold, M. Lock, J. C. Richardson, V. B. Himes, G. Kurtzman, and R. W. Peluso.** 2002. Production of recombinant adeno-associated type 5 (rAAV5) vectors using recombinant herpes simplex viruses containing *rep* and *cap*. Mol. Ther. **6:**510–518.
34. **Yan, Z., R. Zak, G. W. Luxton, T. C. Ritchie, U. Bantel-Schaal, and J. F. Engelhardt.** 2002. Ubiquitination of both adeno-associated virus type 2 and 5 capsid proteins affects the transduction efficiency of recombinant vectors. J. Virol. **76:**2043–2053.
35. **Yang, S., and L. K. Miller.** 1999. Activation of baculovirus very late promoters by interaction with very late factor 1. J. Virol. **73:**3404–3409.
36. **Zadori, Z., J. Szelei, M. C. Lacoste, Y. Li, S. Gariepy, P. Raymond, M. Allaire, I. R. Nabi, and P. Tijssen.** 2001. A viral phospholipase A2 is required for parvovirus infectivity. Dev. Cell **1:**291–302.

ARTICLE

doi:10.1016/j.ymthe.2005.08.009

Viral-Mediated Temporally Controlled Dopamine Production in a Rat Model of Parkinson Disease

Xiao-gang Li,[1,2] Takashi Okada,[2] Mika Kodera,[1] Yuko Nara,[1] Naomi Takino,[1] Chieko Muramatsu,[1] Kunihiko Ikeguchi,[1] Fumi Urano,[3] Hiroshi Ichinose,[3] Daniel Metzger,[4] Pierre Chambon,[4] Imaharu Nakano,[1] Keiya Ozawa,[2,*] and Shin-ichi Muramatsu[1,†]

[1]*Division of Neurology, Department of Medicine, and* [2]*Divison of Genetic Therapeutics, Center for Molecular Medicine, Jichi Medical School, Tochigi 329-0498, Japan*

[3]*Department of Life Science, Tokyo Institute of Technology, Kanagawa 226-8501, Japan*

[4]*Institut de Génétique et de Biologie Moléculaire et Cellulaire, Centre National de la Recherche Scientifique, Institut National de la Santé et de la Recherche Médicale, Université Louis Pasteur, Collège de France, and Institut Clinique de la Souris, 67404 Illkirch Cedex, France*

*To whom correspondence and reprint requests should be addressed at the Division of Genetic Therapeutics, Center for Molecular Medicine, Jichi Medical School, 3311-1 Yakushiji, Minamikawachi, Tochigi 329-0498, Japan. Fax: +81 285 44 8675. E-mail: kozawa@ms.jichi.ac.jp.

†To whom correspondence and reprint requests should be addressed at the Division of Neurology, Department of Medicine, Jichi Medical School, 3311-1 Yakushiji, Minamikawachi, Tochigi 329-0498, Japan. Fax: +81 285 44 5118. E-mail: muramats@ms.jichi.ac.jp.

Available online 22 September 2005

Regulation of gene expression is necessary to avoid possible adverse effects of gene therapy due to excess synthesis of transgene products. To reduce transgene expression, we developed a viral vector-mediated somatic regulation system using inducible Cre recombinase. A recombinant adeno-associated virus (AAV) vector expressing Cre recombinase fused to a mutated ligand-binding domain of the estrogen receptor α (CreER^{T2}) was delivered along with AAV vectors expressing dopamine-synthesizing enzymes to rats of a Parkinson disease model. Treatment with 4-hydroxytamoxifen, a synthetic estrogen receptor modulator, activated Cre recombinase within the transduced neurons and induced selective excision of the tyrosine hydroxylase (TH) coding sequence flanked by loxP sites, leading to a reduction in transgene-mediated dopamine synthesis. Using this strategy, aromatic L-amino acid decarboxylase (AADC) activity was retained so that L-3,4-dihydroxyphenylalanine (L-dopa), a substrate for AADC, could be converted to dopamine in the striatum and the therapeutic effects of L-dopa preserved, even after reduction of TH expression in the case of dopamine overproduction. Our data demonstrate that viral vector-mediated inducible Cre recombinase can serve as an *In vivo* molecular switch, allowing spatial and temporal control of transgene expression, thereby potentially increasing the safety of gene therapy.

Key Words: adeno-associated virus, gene therapy, gene regulation, tamoxifen, Cre recombinase, Parkinson disease, dopamine

INTRODUCTION

Advances in gene transfer methods, in particular the development of improved viral vectors, have expanded the potential of gene therapy to treat a wide range of genetic and acquired diseases. Efficient and long-term expression of therapeutic genes within the central nervous system has been demonstrated in preclinical studies aimed at treating neurodegenerative disorders, including Parkinson disease (PD) [1,2]. PD is a progressive movement disorder characterized by selective degeneration of dopaminergic neurons within the substantia nigra, which project to the striatum. As the dopamine content of the striatum decreases severely, its replacement becomes an important strategy to alleviate motor impairment of the disease. One such strategy is gene therapy to restore the local production of dopamine. Recombinant adeno-associated virus (AAV) vector-mediated gene transfer of dopamine-synthesizing enzymes, such as tyrosine hydroxylase (TH) and guanosine triphosphate cyclohydrolase I (GCH), with or without aromatic L-amino acid decarboxylase (AADC), has induced behavioral recovery in animal models of PD [3–5]. Before clinical trials examining this therapy can commence, however, it is desirable to have a mechanism by which

1525-0016/$30.00

dopamine synthesis can be controlled by regulation of gene expression.

Methods utilizing the properties of bacteriophage P1 site-specific Cre recombinase have been developed in recent years as a means of generating somatic mutations [6]. Regulation of Cre recombinase activity, achieved by fusing Cre with mutated hormone-binding domains of various steroid receptors, has been used in various transgenic applications [7,8]. A chimeric protein known as CreER^{T2}, obtained by fusing Cre to a mutated ligand binding domain of the human estrogen receptor α, is particularly useful. Cell-specific expression of CreER^{T2} in transgenic mice allows efficient tamoxifen-dependent Cre-mediated recombination at loci flanked by loxP sites, without background activity [9]. In the present study, we demonstrate that stereotaxic injection of recombinant AAV vectors expressing dopamine-synthesizing enzymes and CreER^{T2} enables spatiotemporal control of dopamine levels within the brains of rats of a PD model. Our results indicate that these vectors may have a number of applications in gene therapy.

RESULTS

Viral-Mediated Temporally Controlled Cre-Mediated Recombination

We generated AAV vectors expressing either Cre recombinase containing a nuclear localization signal (AAV-Cre) or tamoxifen-dependent Cre recombinase (AAV-CreER^{T2}). To engineer a reporter system, we designed an AAV-EGFP/Red vector to express a destabilized variant of red fluorescent protein (DsRed-Express DR) only after Cre-mediated recombination of a loxP-flanked DNA segment encoding a destabilized, red-shifted variant of green fluorescent protein (d2EGFP) (Fig. 1A). To determine the efficacy of viral-mediated recombination, we infected HEK293 cells with AAV-EGFP/Red and either AAV-Cre or AAV-CreER^{T2} (Fig. 1B). Co-infection of AAV-Cre and AAV-EGFP/Red resulted in expression of DsRed-Express-DR, while only d2EGFP was expressed in control cells infected with AAV-EGFP/Red alone. Co-infection with the reporter vector and AAV-CreER^{T2} induced DsRed-Express-DR expression in almost all 4-hydroxytamoxifen (4-OHT)-treated cells. Although we detected slight background expression of DsRed-Express-DR in the absence of 4-OHT, we observed only a limited number of these cells (<1%), indicating that CreER^{T2} activity is tightly regulated in these virally transduced cells. To test the potential use of AAV-CreER^{T2} *in vivo*, we used stereotaxic injections to deliver AAV-CreER^{T2} into the brains of reporter mice [10]. These mice were engineered to express a red-shifted variant of the wild-type green fluorescent protein (EGFP) only after Cre-mediated excision of a loxP DNA fragment. After 5 consecutive days of 4-OHT treatment (1 mg by intraperitoneal injection), we observed numerous EGFP-expressing cells in AAV-injected brains, all of which coexpressed Cre recombinase (Fig. 1C). In the absence of treatment with 4-OHT, only a few cells (<0.1% of Cre-positive cells) expressed EGFP in the vicinity of AAV-CreER^{T2}-injected sites (data not shown). These data indicate that floxed DNA segments are efficiently excised *in vivo* by combining AAV-CreER^{T2} injection with 4-OHT treatment.

Temporally Controlled Reduction of Dopamine Synthesis

We generated AAV vectors expressing each of the three dopamine-synthesizing enzymes (TH, AADC, and GCH). In the TH-expressing vector, two loxP sites flanked the TH coding sequence (AAV-floxed TH). We infected HEK293 cells with these dopamine-synthesizing vectors (AAV-floxed TH, AAV-AADC, and AAV-GCH) in combination

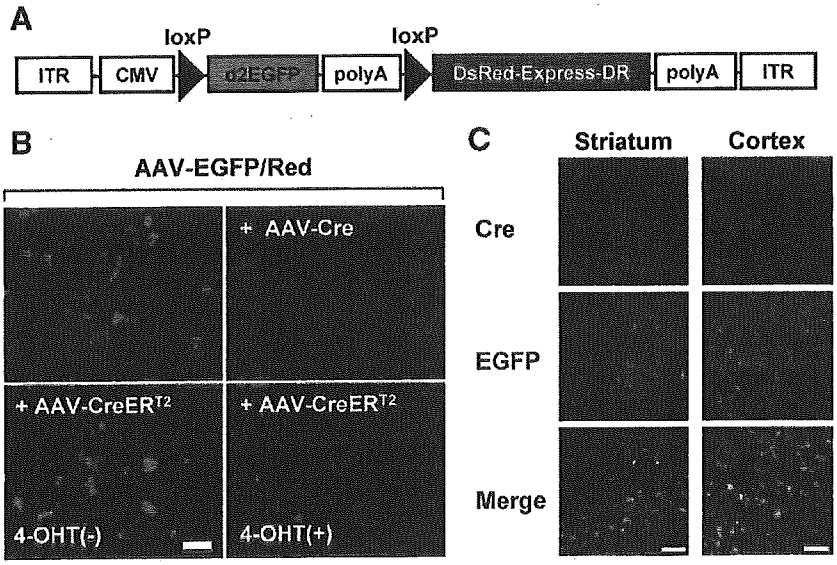

FIG. 1. Viral vector-mediated Cre-dependent floxed DNA excision. (A) Illustration of the AAV-EGFP/Red vector construct. A DsRed-Express-DR marker was placed downstream of the d2EGFP marker with a SV40 poly(A) sequence flanked by loxP sites. ITR, inverted terminal repeat; CMV, human cytomegalovirus immediate-early promoter followed by the first intron of human growth hormone. (B) 4-OHT-induced Cre-dependent recombination. HEK293 cells were infected with AAV-EGFP/Red and either AAV-Cre or AAV-CreER^{T2}. 4-OHT was added to the medium 5 h after infection. Fluorescence was observed 48 h after infection. Bar, 40 μm. (C) EGFP expression in the AAV-CreER^{T2}-injected striatum and cortex of transgenic mice. 4-OHT (1 mg) was administered intraperitoneally 1 week after vector injection every day for 5 days until the mice were killed. In these mice, the stop fragment was flanked by loxP sites and placed between the EGFP sequence and the *Gt(ROSA)26Sor* promoter. Bar, 40 μm.

doi:10.1016/j.ymthe.2005.08.009

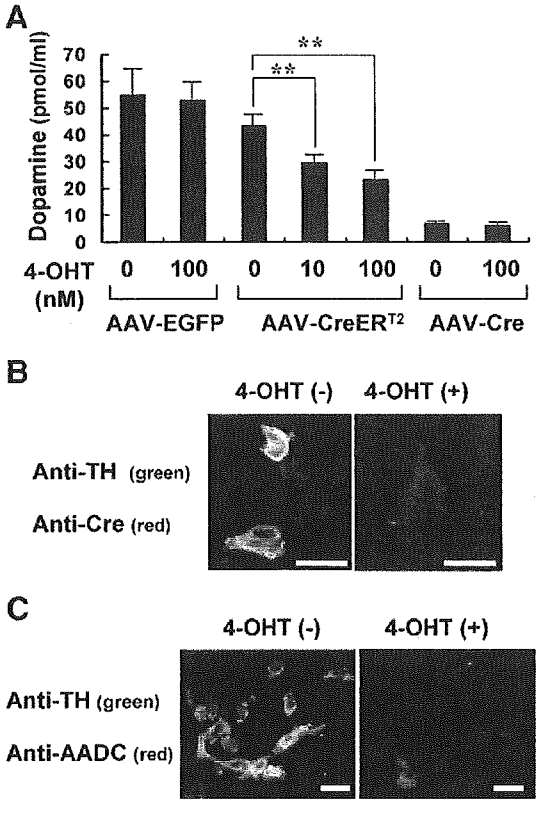

FIG. 2. Reduced dopamine synthesis after 4-OHT-induced ablation of a floxed TH transgene. HEK293 cells were infected with dopamine-synthesizing vectors (AAV-floxed TH, AAV-AADC, and AAV-GCH) in combination with AAV-CreER^{T2} or control vectors. (A) Dopamine content in the culture medium was significantly reduced in the presence of 4-OHT. $^{**}P < 0.01$, $n = 4$. (B) TH (green) and CreER^{T2} (red) immunocytochemistry was performed 48 h after vector infection. Yellow fluorescence in the merged image indicates colocalization. In the presence of 4-OHT, CreER^{T2} translocated to the nucleus. TH was not expressed in cells positive for nuclear CreER^{T2}. Bar, 20 μm. (C) TH (green) and AADC (red) immunocytochemistry. Note the reduced number of TH-positive cells in the presence of 4-OHT. Bar, 20 μm.

with AAV-CreER^{T2} or control vectors. We found that treatment with 4-OHT significantly reduced dopamine synthesis (Fig. 2A). Immunocytochemistry demonstrated coexpression of TH and CreER^{T2} in the cytoplasm in the absence of 4-OHT and an absence of TH expression when CreER^{T2} was translocated into the nucleus in the presence of 4-OHT (Fig. 2B). The expression of AADC was not reduced by the presence of 4-OHT (Fig. 2C). Dual labeling showed that more than 80% of the TH-immunoreactive (TH-IR) cells were also positive for AADC (251 of 300) and Cre (242 of 300) in the absence of 4-OHT-treatment.

Reduction of Dopamine Production in a Rat Model

We next tested whether the vector-mediated Cre-dependent regulation of transgene expression observed in culture could be extended to animal models. We obtained hemiparkinsonian rats by injecting a selective neurotoxin, 6-hydroxydopamine (6-OHDA), into the left medial forebrain bundle. The animals then received a mixture of AAV-CreER^{T2}, AAV-floxed TH, AAV-AADC, and AAV-GCH into their lesioned striatum, after which two-thirds were further treated with 4-OHT (4 mg/kg by intraperitoneal injection for 5 days) during the course of experimentation. Control rats were injected with AAV-LacZ alone or with AAV-Cre plus AAV-floxed TH, AAV-AADC, and AAV-GCH. To evaluate abnormal motor functions associated with depletion of dopamine in the striatum, we repeated quantification of apomorphine-induced rotation, as well

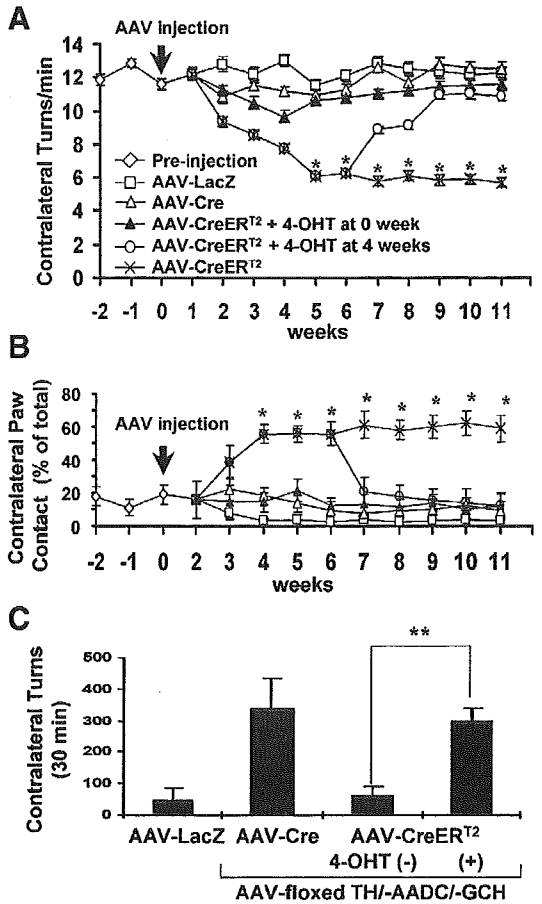

FIG. 3. Temporal control of dopamine synthesis in a rat model of PD transduced with AAV vectors. Sixty hemiparkinsonian rats were generated by 6-OHDA injection. Thirty-six received a mixture of AAV-CreER^{T2}, AAV-floxed TH, AAV-AADC, and AAV-GCH, after which they were divided into three groups of 12. Two of the groups were treated with 4-OHT (4 mg/kg by intraperitoneal injection for 5 days), at the same time or 4 weeks after vector injection. Control PD rats were injected with AAV-LacZ alone ($n = 12$) or AAV-Cre ($n = 12$), instead of AAV-CreER^{T2} with AAV-floxed TH, AAV-AADC, and AAV-GCH. (A) The total number of complete body turns induced by apomorphine was counted for each rat, and (B) spontaneous limb use was scored using the cylinder test. $^{*}P < 0.05$. (C) Efficient conversion of L-dopa to dopamine by AADC. L-Dopa (5 mg/kg) was administered to 4-OHT-treated rats and AAV-Cre-injected rats. Contralateral turning in response to L-dopa was counted for 30 min. $^{**}P < 0.01$. Legend symbols are as shown in A and B.

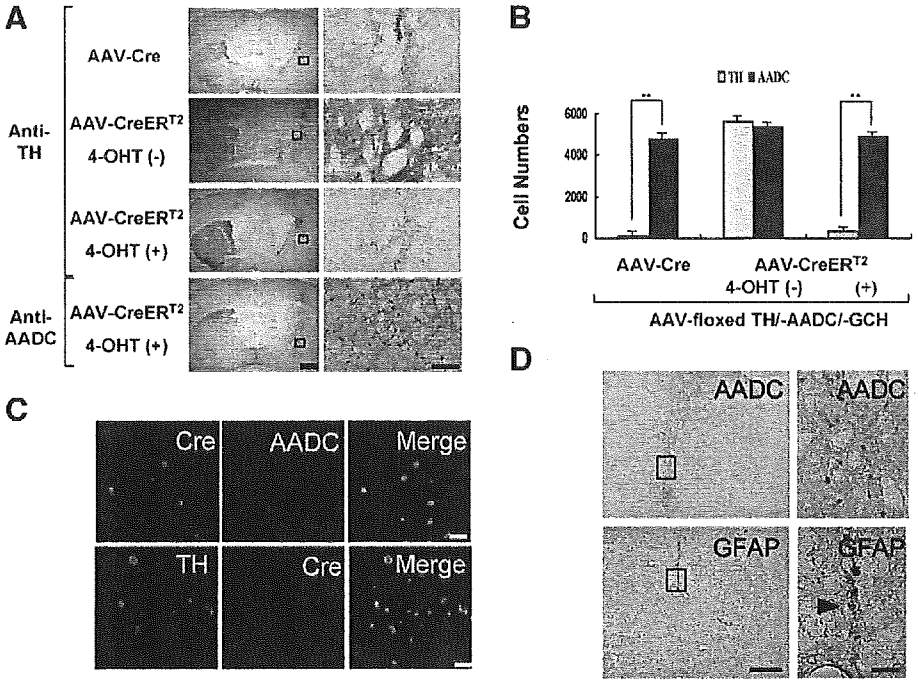

FIG. 4. Selective ablation of the TH transgene induced by treatment with 4-OHT. (A) Immunohistochemical staining for TH or AADC in the brains of 6-OHDA-lesioned rats 12 weeks after stereotaxic injection of AAV-Cre or AAV-CreER^{T2}, with or without 4-OHT treatment. AAV vectors were injected into the lesioned side of the striatum (right side of the photos). High-power-magnified images of the vector injection sites (squares in the left column) are shown in the right column. Representative photographs are also shown. Bar, 1.5 mm (left column), 100 μm (right column). (B) Number of immunoreactive (IR) cells against TH or AADC in the multiple AAV vector-injected striatum. The number of cells in 11 sections per rat (n = 3 for each group) was counted. The numbers of TH-IR cells and AADC-IR cells in AAV-CreER^{T2}-injected rats given 4-OHT 0 or 4 weeks after vector injection were indistinguishable and the results pooled for comparison with other groups. $^{**}P < 0.01$. (C) Efficient cotransduction of AAV vectors, as determined by dual immunofluorescence staining of the 6-OHDA-lesioned striatum. The majority of Cre-IR cells were also positive for TH and AADC. Bar, 20 μm. (D) Parallel striatal sections immunostained for glial fibrillary acidic protein (GFAP) or AADC. Striatal cells were transduced without obvious reactive astrocytosis. Residual hemosiderin was observed along the needle tract. On the right are magnified views of the boxes on the left. Bars: 0.5 mm, left; 50 μm, right.

as the cylinder test, weekly until the rats were killed. In the absence of 4-OHT, we observed behavioral recovery in rats that received both AAV-CreER^{T2} and AAV vectors expressing dopamine-synthesizing enzymes. Following 4-OHT treatment, these rats regressed, demonstrating impaired behavior (Figs. 3A and 3B). No recovery occurred in AAV-CreER^{T2}-injected rats treated with 4-OHT at the same time as vector injection or in AAV-Cre- or AAV-LacZ-injected rats. Contralateral turning in response to L-3,4-dihydroxyphenylalanine (L-dopa, 5 mg/kg) was not significantly reduced in 4-OHT-treated rats or AAV-Cre injected rats, indicating efficient conversion of L-dopa to dopamine in the striatum due to preservation of AADC activity (Fig. 3C).

Immunohistochemistry showed fewer TH-IR cells in rats that received AAV-Cre or AAV-CreER^{T2} plus 4-OHT, compared to injected rats not treated with 4-OHT (Figs. 4A and 4B). The numbers of AADC-immunoreactive cells,

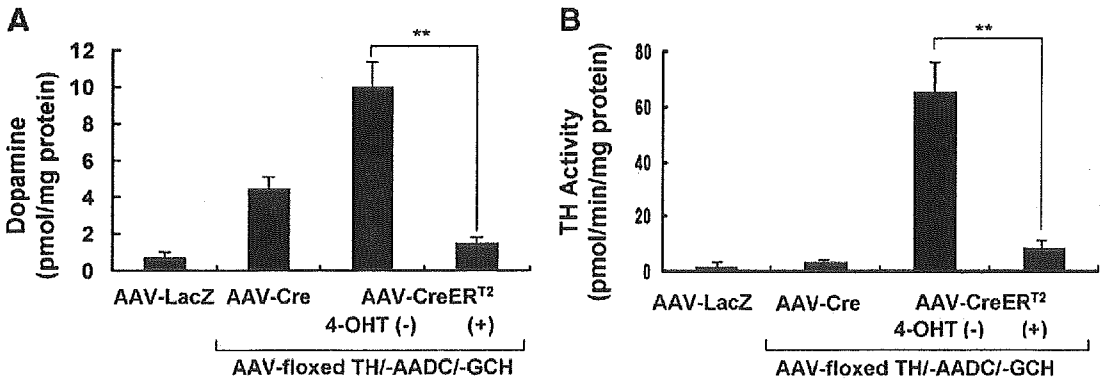

FIG. 5. Reduction of dopamine synthesis in 4-OHT-treated rats. Significantly less (A) dopamine content and (B) TH activity were observed in the lesioned striatum of 4-OHT-treated rats 12 weeks after vector injection, compared to 4-OHT-untreated rats. $^{**}P < 0.01$, n = 4.

doi:10.1016/j.ymthe.2005.08.009

however, did not differ significantly between 4-OHT-treated and untreated rats. We roughly estimated the number of transduced cells in the striatum at 5×10^4 based on cell counts performed on the tissue sections. This efficiency of transduction is sufficient to parallel the functional effects on behavior observed in other studies [3,5,11]. Double-labeling with both anti-Cre and anti-TH antibodies, or with anti-Cre and anti-AADC antibodies, showed that more than 80% of Cre-immunoreactive cells were also positive for TH (164 of 200) and AADC (176 of 200) in three 4-OHT-untreated rats (Fig. 4C). Immunostaining for glial fibrillary acidic protein (GFAP) or AADC in parallel sections demonstrated transduction of striatal cells without obvious reactive astrocytosis (Fig. 4D). Dopamine content (Fig. 5A) and TH activity (Fig. 5B) within the lesioned striatum were significantly lower in 4-OHT-treated compared to untreated rats. Dopamine levels in the transduced striatum in the 4-OHT-treated and untreated rats were 0.66 and 4.3%, respectively, those of the unlesioned striatum. Unlike primary dopamine in the nigrostriatal system, which is stored in synaptic vesicles, genetically produced dopamine in the lesioned striatum might be readily metabolized without storage. Since the dopamine level in the lesioned side of AAV-LacZ-injected rats was much lower (0.3%), a 10-fold increase in dopamine level after triple transduction with TH, AADC, and GCH genes caused a remarkable therapeutic effect. Average TH activity, measured in terms of L-dopa production (pmol/min/mg protein), reached 51.6% that of the normal striatum (65.9 ± 11.0 versus 127.7 ± 3.7) in rats transduced with dopamine-synthesizing enzymes. In 4-OHT-treated rats, TH activity fell to 10.8% of normal (13.8 ± 4.1).

DISCUSSION

Our results show efficient viral vector-mediated delivery of tamoxifen-dependent $CreER^{T2}$ recombinase into rodent brains and that transgenic floxed sequences can be deleted in a temporally controlled manner. In a rat model of PD, recombinant AAV vector-mediated delivery of $CreER^{T2}$ into the striatum enabled 4-OHT-induced excision of a floxed TH transgene, resulting in reduced virally mediated dopamine synthesis. We targeted TH, a rate-limiting enzyme for dopamine biosynthesis that converts dietary L-tyrosine to L-dopa. Using this strategy, AADC activity was retained so that L-dopa, a substrate for AADC capable of crossing the blood–brain barrier, could be converted to dopamine in the striatum. Thus, in clinical situations, the therapeutic effects of orally administered L-dopa would likely be preserved, even after 4-OHT treatment to reduce TH expression in cases of dopamine overproduction [11]. Although transduction with AADC alone, in combination with oral administration of L-dopa, might not achieve continuous delivery of L-dopa, in contrast to that which could potentially be achieved with triple transduction of TH, AADC, and GCH, dopamine production could be regulated by altering the dose of L-dopa, thereby providing a safer option for gene therapy. We previously demonstrated that dopamine synthesis was enhanced (greater than fivefold) after systemic administration of L-dopa in AAV-TH/-AADC/-GCH-injected striatum in the primate model of PD using *in vivo* dialysis [4]. A phase I clinical trial involving gene transfer of AADC alone is currently under way.

AAV vectors are powerful tools by which to deliver therapeutic genes into the mammalian brain. Many striatal neurons of rodents and nonhuman primates are transduced with AAV vectors via stereotaxic injection, and long-term gene expression has been achieved without substantial toxicity or immune response [2,12]. AAV vectors have safety advantages over other viral vectors when it comes to *in vivo* gene delivery, since they are derived from nonpathogenic wild-type viruses. Moreover, most recombinant AAVs are present in cells as episomes, thus reducing the probability of insertional activation of oncogenes, compared to retroviruses, which integrate into host chromosomes [13]. Although it is difficult to use a single AAV vector for multiple gene transfer due to its limited packaging capacity (<5 kb), a single cell can be simultaneously transduced with multiple AAV vectors. In the present study, dual immunofluorescence staining showed efficient cotransduction of cells with different AAV vectors in the rat striatum, a finding consistent with that which we observed in a previous study [5].

Gene therapy strategies for the treatment of PD using AAV vectors include gene delivery of dopamine-synthesizing enzymes into the striatum to restore dopamine production, as well as gene delivery of neuroprotective molecules, such as glial cell line-derived neurotrophic factor, to block or slow down further degeneration [14]. In addition, AAV vectors harboring genes encoding neurotrophic factors might be delivered by intramuscular administration in an attempt to protect spinal motoneurons in patients suffering from amyotrophic lateral sclerosis [15–17]. Although no adverse effects due to overexpression of transgenes have been reported in animals to date, it is necessary to develop vectors that allow for regulation of transgene expression, thus avoiding transgene overexpression. In PD, overproduction of dopamine has the potential to cause dyskinesia or hallucinations, and sustained exposure to high concentrations of neurotrophic factors could result in tumor formation.

Inducible Cre recombinases have been used to generate a number of conditional knockout mice. They are invaluable tools for investigators studying the role of gene function in development, as well as a number of physiological and pathological processes.. The tamoxifen-dependent $CreER^{T2}$ recombinase has proven particularly helpful [9,18,19]. It has been shown that 4-OHT does not alter dopamine content within the striatum in mice [20],

and we did not observe any adverse effects of 4-OHT treatment in the present experiment. In addition, tamoxifen, which is metabolized by the liver into 4-OHT, has neuroprotective effects [21,22]. Thus, the CreER^{T2} system might be useful for gene therapy in the treatment of neurological diseases.

We have expanded upon the use of inducible Cre recombinase technology to regulate transgene expression using an AAV vector-mediated gene delivery system. Recently, a viral vector-mediated RNA interference (RNAi) approach has been developed and localized gene knockdown achieved in the adult brain [23–25]. Although RNAi-mediated suppression of gene function has a wide variety of applications, more specific and inducible transgene silencing can be achieved with AAV-CreER^{T2}. Selective ablation of floxed transgenes reduces the possibility of down-regulation of normal cellular proteins. This system works as a molecular switch, increasing the safety of long-acting gene therapy by avoiding or minimizing side effects due to overproduction of the protein product and by providing the ability to shut down expression if toxicities are encountered or treatment is completed. The ability to restrict somatic recombination of transgenes spatially and temporally has a wide range of applications, in both gene therapy and biological study requiring somatic genetic manipulation.

Materials and Methods

AAV vector production. The AAV vector plasmids contained an expression cassette with a human cytomegalovirus immediate-early promoter (CMV promoter), followed by the first intron of human growth hormone, target cDNA, and a simian virus 40 polyadenylation signal sequence (SV40 poly(A)), between the inverted terminal repeats of the AAV-2 genome. The plasmids pAAV-LacZ, pEGFP, pAAV-AADC, pAAV-GCH, pCre, and pCreER^{T2} contained the cDNAs of LacZ, EGFP, human AADC, human GCH, Cre recombinase with a nuclear localization signal [26], and Cre recombinase fused to a mutated form of the ligand-binding domain of estrogen receptor α (CreER^{T2})[27], respectively. The plasmid pAAV-floxed TH contained human TH1 cDNA flanked by two loxP sequences between the CMV promoter and the SV40 poly(A). To generate pAAV-EGFP/Red, a DNA fragment containing d2EGFP (BD Biosciences, San Jose, CA, USA) and the SV40 poly(A) was flanked by loxP sequences and inserted between the CMV promoter and DsRed-Express-DR (BD Biosciences). The two helper plasmids, pHLP19 and pladeno1 (Avigen, Alameda, CA, USA), harbored the AAV *rep* and *cap* genes, as well as the *E2A*, *E4*, and *VA RNA* genes of the adenovirus genome, respectively. HEK293 cells were cotransfected by the calcium phosphate coprecipitation method with the vector plasmid, pHLP19, and pladeno1. The AAV vectors were then harvested and purified by two rounds of continuous iodoxale ultracentrifugations. Vector titers were determined by quantitative DNA dot-blot hybridization or by quantitative PCR of DNase I-treated vector stocks. We routinely obtained 10^{12} to 10^{13} vector genome copies (vg).

In vitro transduction. HEK293 cells were seeded at 3×10^5 cells/well in six-well plates. After 24 h, cells were infected with appropriate combinations of AAV vectors (5×10^9 vg per vector). 4-OHT was added to the culture medium at a concentration of 10 or 100 nM at 5 h after infection. Culture medium was collected for dopamine assay 48 h after infection and the cells were fixed for immunostaining.

AAV injections. All animal experiments were performed in accordance with the institutional guidelines. Three B6,129-*Gt(ROSA))26Sor*^{tm2Sho}/J mice (The Jackson Laboratory, Bar Harbor, ME, USA) [10] were stereotaxically injected into the caudoputaminal unit or cerebral cortex with 1×10^9 vg (1 μl) of AAV-CreER^{T2}. After 1 week, 4-OHT (1 mg) was administered intraperitoneally every day for 5 days, after which 2 of the mice were killed. One mouse that did not receive 4-OHT treatment was killed as a control. Creation of PD model rats and stereotaxic injections of AAV vectors were carried out as previously described [5]. Briefly, 60 male albino Wistar rats (weighing 200–250 g) were unilaterally lesioned at the left medial forebrain bundle (coordinates AP −4.3 mm and ML 1.6 mm, relative to the bregma, and DV −7.8 mm relative to the dura, with the incisor bar set 3.3 mm below the interaural line) with 4 μl of 4.5 mg/ml 6-OHDA HBr (Sigma, St. Louis, MO, USA) in 0.02% ascorbate saline prior to intrastriatal transduction. These rats were stereotaxically injected with AAV vectors (5×10^7 vg per site for each vector) at three sites in the lesioned striatum (coordinates relative to the bregma and dura, AP +1.5, +1.0, and +0.5 mm; ML 2.6, 3.0, and 3.2 mm; DV −5.2 mm). Forty-eight rats were injected with a 1:1:1 mixture of AAV-floxed TH, AAV-AADC, and AAV-GCH plus AAV-Cre (n = 12) or AAV-CreER^{T2} (n = 36). Twelve rats received AAV-LacZ alone as a control. Among the AAV-CreER^{T2}-treated rats, 24 were intraperitoneally injected with 4-OHT (4 mg/kg) for 5 consecutive days, starting either at the same time as or 4 weeks after vector injection.

Behavioral testing. The rats were tested weekly for rotational behavior and spontaneous limb use, as described previously [28]. The total number of complete body turns was counted during an observation period of ≥60 min following intraperitoneal injection of apomorphine HCl (0.1 mg/kg; Sigma). Only those animals exhibiting seven or more contralateral rotations/min in a 60-min period at 4 weeks after the 6-OHDA injection were included in further analysis. Spontaneous limb use was scored according to the cylinder test method [29]. Rats were placed in a clear glass cylinder large enough to ensure free movement. After they had performed 10 rears during which they were observed to place at least one paw on the cylinder wall, the number of times both forepaws contacted the wall of the cylinder was counted until at least 20 contacts were made. Data indicating the number of times a contralateral forepaw made contact with the wall are expressed as a percentage of the total. We also evaluated rotational behavior in response to a low dose of L-dopa methyl ester (5 mg/kg; Sigma) coadministered with 2.5 mg/kg of a peripheral decarboxylase inhibitor (benserazide hydrochloride; Sigma) 10 weeks after AAV injection.

Biochemical assays. Levels of dopamine in the cell culture medium (n=4 for each group) and within the brain samples (n=4 for each group) were determined by high-performance liquid chromatography (HPLC), as previously described [5]. Rats were killed by decapitation under sodium pentobarbital anesthesia 12 weeks after vector injection, after which their brains were immediately dissected and placed on dry ice. The striatum was punched out bilaterally using a sharp-edged, stainless steel tube. Wet tissue samples were weighed and stored at −80°C until subsequent analysis. Tissues were homogenized in 20 volumes of homogenization buffer and then mixed immediately with 0.76 M perchloric acid prior to centrifugation at 15,000*g* for 10 min. After the supernatant was neutralized with sodium acetate, the samples were analyzed by HPLC analysis. Determination of TH activity was based on the formation of L-dopa from L-tyrosine, as demonstrated by HPLC electrochemical detection. The reaction mixture contained 200 mM sodium acetate buffer (pH 6.0), 100 mM 2-mercaptoethanol, 0.2 mg/ml catalase, 0.2 mM L-tyrosine, and 1 mM tetrahydrobiopterin. The mixture was incubated for 10 min at 37°C. The reaction was stopped by adding perchloric acid, and L-dopa was extracted using an alumina column [30].

Immunostaining of cultured cells and brain sections. Cultured cells were fixed in 4% paraformaldehyde (PFA) in PBS. Brains were perfused with 4% PFA, soaked in 30% sucrose, and dissected into coronal sections (30 μm). The following primary antibodies were used: TH monoclonal (1:800 or 1:8000; DiaSorin, Stillwater, MN, USA) or polyclonal (1:10,000; provided by Ikuko Nagatsu, Fujita Health University, Japan), AADC polyclonal (1:10,000; I. Nagatsu), Cre recombinase monoclonal (1:500; Covance, Princeton, NJ, USA) or polyclonal (1:500; Covance), GFP polyclonal (1:200; BD Biosciences or Chemicon, Temecula, CA, USA), DsRed

doi:10.1016/j.ymthe.2005.08.009

polyclonal (1:1000; BD Biosciences), and GFAP (1:1000; Chemicon). Appropriate fluorescence-tagged (Invitrogen, Carlsbad, CA, USA) or biotinylated (Vector Laboratories, Burlingame, CA, USA) secondary antibodies were used for visualization. Immunoreactivity was assessed under microscopy (Axioplan, Zeiss, Germany) or confocal laser scanning microscopy (TCS NT; Leica Microsystems, Germany). To analyze quantitatively the numbers of TH-positive neurons and AADC-positive neurons, every 10th 30-μm section (total of 11 sections) covering a 3-mm thickness from each animal ($n = 3$ per group) was examined. Coexpression efficacy was analyzed by dual immunofluorescence staining.

Statistical analysis. One-way analysis of variance (ANOVA) was performed to determine differences in dopamine levels, as well as TH activity, followed by Tukey's test (StatView 5.0 software; Abacus). Behavioral changes were analyzed by a repeated measure ANOVA, followed by Tukey's test, with $P < 0.05$ considered statistically significant. Results are presented as means ± SEM.

ACKNOWLEDGMENTS

We thank Avigen, Inc., for providing the AAV vector production system. This work was supported by grants from the Ministry of Education, Science, Sports, and Culture, as well as by funds made available by the Japanese Government for a High-Tech Research Center Project for Private Universities (2003–2005) and a University–Industry Joint Research Project (2003–2005). In addition, we received grants from the Japan Ministry of Health, Labor, and Welfare; a grant from The Ministere de l'Education Nationale, de l'Enseignement Superieur et de la Recherche; and funds from The Cell Science Research Foundation, the Centre National de la Recherche Scientifique, the Institut National de la Santé et de la Recherche Médicale, and the Collège de France.

RECEIVED FOR PUBLICATION MAY 14, 2005; REVISED JULY 26, 2005; ACCEPTED AUGUST 1, 2005.

REFERENCES

1. Burton, E. A., Glorioso, J. C., and Fink, D. J. (2003). Gene therapy progress and prospects: Parkinson's disease. *Gene Ther.* **10:** 1721–1727.
2. Muramatsu, S., *et al.* (2003). Adeno-associated viral vectors for Parkinson's disease. *Int. Rev. Neurobiol.* **55:** 205–222.
3. Mandel, R. J., *et al.* (1998). Characterization of intrastriatal recombinant adeno-associated virus-mediated gene transfer of human tyrosine hydroxylase and human GTP-cyclohydrolase I in a rat model of Parkinson's disease. *J. Neurosci.* **18:** 4271–4284.
4. Muramatsu, S., *et al.* (2002). Behavioral recovery in a primate model of Parkinson's disease by triple transduction of striatal cells with adeno-associated viral vectors expressing dopamine-synthesizing enzymes. *Hum. Gene Ther.* **13:** 345–354.
5. Shen, Y., *et al.* (2000). Triple transduction with adeno-associated virus vectors expressing tyrosine hydroxylase, aromatic-L-amino-acid decarboxylase, and GTP cyclohydrolase I for gene therapy of Parkinson's disease. *Hum. Gene Ther.* **11:** 1509–1519.
6. Rajewsky, K., *et al.* (1996). Conditional gene targeting. *J. Clin. Invest.* **98:** 600–603.
7. Branda, C. S., and Dymecki, S. M. (2004). Talking about a revolution: the impact of site-specific recombinases on genetic analyses in mice. *Dev. Cell* **6:** 7–28.
8. Metzger, D., and Feil, R. (1999). Engineering the mouse genome by site-specific recombination. *Curr. Opin. Biotechnol.* **10:** 470–476.
9. Metzger, D., *et al.* (2003). Targeted conditional somatic mutagenesis in the mouse: temporally-controlled knock out of retinoid receptors in epidermal keratinocytes. *Methods Enzymol.* **364:** 379–408.
10. Mao, X., *et al.* (2001). Activation of EGFP expression by Cre-mediated excision in a new ROSA26 reporter mouse strain. *Blood* **97:** 324–326.
11. Sanchez-Pernaute, R., Harvey-White, J., Cunningham, J., and Bankiewicz, K. S. (2001). Functional effect of adeno-associated virus mediated gene transfer of aromatic L-amino acid decarboxylase into the striatum of 6-OHDA-lesioned rats. *Mol. Ther.* **4:** 324–330.
12. Tenenbaum, L., *et al.* (2004). Recombinant AAV-mediated gene delivery to the central nervous system. *J. Gene Med.* 6(Suppl. 1): S212–S222.
13. McCarty, D. M., Young, S. M., Jr., and Samulski, R. J. (2004). Integration of adeno-associated virus (AAV) and recombinant AAV vectors. *Annu. Rev. Genet.* **38:** 819–845.
14. Hurelbrink, C. B., and Barker, R. A. (2004). The potential of GDNF as a treatment for Parkinson's disease. *Exp. Neurol.* **185:** 1–6.
15. Azzouz, M., *et al.* (2004). VEGF delivery with retrogradely transported lentivector prolongs survival in a mouse ALS model. *Nature* **429:** 413–417.
16. Kaspar, B. K., *et al.* (2003). Retrograde viral delivery of IGF-1 prolongs survival in a mouse ALS model. *Science* **301:** 839–842.
17. Wang, L. J., *et al.* (2002). Neuroprotective effects of glial cell line-derived neurotrophic factor mediated by an adeno-associated virus vector in a transgenic animal model of amyotrophic lateral sclerosis. *J. Neurosci.* **22:** 6920–6928.
18. Imai, T., *et al.* (2004). Peroxisome proliferator-activated receptor gamma is required in mature white and brown adipocytes for their survival in the mouse. *Proc. Natl. Acad. Sci. USA* **101:** 4543–4547.
19. Simon, D., *et al.* (2004). Friedreich ataxia mouse models with progressive cerebellar and sensory ataxia reveal autophagic neurodegeneration in dorsal root ganglia. *J. Neurosci.* **24:** 1987–1995.
20. Kuo, Y. M., *et al.* (2003). 4-Hydroxytamoxifen attenuates methamphetamine-induced nigrostriatal dopaminergic toxicity in intact and gonadectomized mice. *J. Neurochem.* **87:** 1436–1443.
21. Ciriza, I., *et al.* (2004). Selective estrogen receptor modulators protect hippocampal neurons from kainic acid excitotoxicity: differences with the effect of estradiol. *J. Neurobiol.* **61:** 209–221.
22. Obata, T., and Kubota, S. (2001). Protective effect of tamoxifen on 1-methyl-4-phenylpyridine-induced hydroxyl radical generation in the rat striatum. *Neurosci. Lett.* **308:** 87–90.
23. Harper, S. Q., *et al.* (2005). RNA interference improves motor and neuropathological abnormalities in a Huntington's disease mouse model. *Proc. Natl. Acad. Sci. USA* **102:** 5820–5825.
24. Hommel, J. D., *et al.* (2003). Local gene knockdown in the brain using viral-mediated RNA interference. *Nat. Med.* **9:** 1539–1544.
25. Xia, H., *et al.* (2004). RNAi suppresses polyglutamine-induced neurodegeneration in a model of spinocerebellar ataxia. *Nat. Med.* **10:** 816–820.
26. Kalderon, D., Roberts, B. L., Richardson, W. D., and Smith, A. E. (1984). A short amino acid sequence able to specify nuclear location. *Cell* **39:** 499–509.
27. Feil, R., Wagner, J., Metzger, D., and Chambon, P. (1997). Regulation of Cre recombinase activity by mutated estrogen receptor ligand-binding domains. *Biochem. Biophys. Res. Commun.* **237:** 752–757.
28. Wang, L., *et al.* (2002). Delayed delivery of AAV-GDNF prevents nigral neurodegeneration and promotes functional recovery in a rat model of Parkinson's disease. *Gene Ther.* **9:** 381–389.
29. Schallert, T., *et al.* (2000). CNS plasticity and assessment of forelimb sensorimotor outcome in unilateral rat models of stroke, cortical ablation, parkinsonism and spinal cord injury. *Neuropharmacology* **39:** 777–787.
30. Nagatsu, T., Oka, K., and Kato, T. (1979). Highly sensitive assay for tyrosine hydroxylase activity by high-performance liquid chromatography. *J. Chromatogr.* **163:** 247–252.

HUMAN GENE THERAPY 16:1413–1421 (December 2005)

Repair of Articular Cartilage Defect by Intraarticular Administration of Basic Fibroblast Growth Factor Gene, Using Adeno-Associated Virus Vector

ATSUO HIRAIDE,[1] NAOKI YOKOO,[1] KE-QIN XIN,[2] KENJI OKUDA,[2] HIROAKI MIZUKAMI,[3] KEIYA OZAWA,[3] and TOMOYUKI SAITO[1]

ABSTRACT

The objective of this study was to establish the potency of adeno-associated virus (AAV) as a viral vector to transport the basic fibroblast growth factor (bFGF) gene into synovial tissue, and to evaluate the consequent repair of articular cartilage defects. In the *in vitro* study, LacZ- and bFGF-encoding genes were transduced into rabbit synoviocytes by recombinant adeno-associated virus (AAV) vector, and the cells were cultured for 2 weeks. The percentage of successfully transduced LacZ-positive cells was assessed by 5-bromo-4-chloro-3-indolyl-β-D-galactopyranoside staining, and the concentration of bFGF in the culture supernatant was confirmed by bFGF-specific enzyme-linked immunosorbent assay. In the *in vivo* study, 12- to 14-week-old Japanese white rabbits (all female) were used. AAV-bFGF was administered into an artificially created full-thickness defect (5 mm in diameter and 3 mm deep) in the patellar groove of the distal femur. Cartilage repair was subsequently monitored at 4, 8, and 12 weeks, by macroscopic and histological examination, and results were graded on the basis of semiquantitative scores. *lacZ* gene expression in synoviocytes reached more than 93% within the first 2 weeks, and the mean bFGF concentration in the culture supernatant of the bFGF gene-transduced group was significantly increased ($p < 0.01$). Semiquantitative macroscopic and histological assessment indicated that the average score was significantly better in the bFGF-transduced group throughout the observation period, suggesting better cartilage repair. These results demonstrate that gene transfer into synoviocytes, using the AAV vector, was a potent method of gene transduction. Moreover, after intraarticular administration of AAV-bFGF, constant expression of bFGF in the knee joints resulted in substantial cartilage regeneration that, with further long-term study, could possibly merit consideration for clinical application.

OVERVIEW SUMMARY

Adeno-associated virus (AAV) is well known as a dynamic gene transporter with a number of biological advantages, such as a lack of virulence in the wild type and the ability to maintain continuous local expression of the therapeutic gene. It is also known that integration of the basic fibroblast growth factor (bFGF) gene into tissues, such as synoviocytes, by intraarticular administration has the potential to produce lasting expression and sustained secretion of the growth factor, leading to regeneration of cartilage. In this study, using AAV as a viral vector, we have demonstrated that the bFGF cache was notably enlarged in bFGF-transduced synoviocytes, using rabbits as laboratory animals, *in vitro* and *in vivo*. Our study clearly demonstrates that, with intraarticular administration of AAV-bFGF, a high efficiency of transduction can be obtained with a complementary elevated level of cartilage repair that has definite clinical potential in the treatment of cartilaginous diseases.

INTRODUCTION

ARTICULAR CARTILAGE is a highly differentiated tissue with limited capacity for self-repair. Thus, it is extremely vulnerable to traumatic erosion or defect, and osteoarthritic degeneration, which often lead to joint dysfunction associated with pain and/or limitation in range of motion. Current treat-

[1]Department of Orthopedic Surgery and [2]Department of Bacteriology, Yokohama City University School of Medicine, Yokohama, Japan.
[3]Division of Genetic Therapeutics, Center for Molecular Medicine, Jichi Medical School, Tochigi, Japan.

ment for osteoarthritis consists of (1) conservative therapy such as use of short-acting nonsteroidal antiinflammatory drugs, intraarticular injection of steroids, and/or other agents such as hyaluronic acid, and (2) surgical intervention such as high-tibial osteotomy and surface replacement. However, these treatments do not always relieve joint pain completely and, moreover, do not aid regeneration of cartilage. Thus, cartilage repair at an early stage, if possible, would appear to be a more fundamental method of preventing the irreversible detrimental outcome of total joint failure. In the past, some efforts have been made to repair osteochondral defects by methods such as treatment by transplantation of cultured chondrocytes (Brittberg *et al.*, 1994) or, more recently, *ex vivo* transplantation of cultured chondrocytes (Yokoo *et al.*, 2005); however, both methods had their disadvantages. In the former, when a large quantity of chondrocytes from normal articular cartilage is required, donor sites have limited capacity to provide them. The latter study overcomes the donor problem, but presents other disadvantages such as infection during culture, and complexity of the method itself.

Other studies have reported that basic fibroblast growth factor (bFGF) is one of the most potent substances for proliferation and differentiation of chondrocytes, triggering a cascade of events in the cartilage repair process (Cuevas *et al.*, 1988; Hunziker and Rosenberg, 1996; Shida *et al.*, 1996; Weisser *et al.*, 2001). With this knowledge, it can be hypothesized that to maintain a certain level of bFGF for a specific time period at a chondral defect site could prove to be advantageous. Application of gene therapy could provide the answer, and cases of cartilage repair using naked DNA or viral vectors as gene transporters have been reported (Arai *et al.*, 1997; Baragi *et al.*, 1997; Kang *et al.*, 1997; Doherty *et al.*, 1998).

However, such gene transduction has also proved problematic, with a low level of transduction efficiency, lack of capacity to maintain long-term expression of the therapeutic gene, and difficulty in maintaining adequate safety levels. In other studies, the adeno-associated virus (AAV) has been recognized as a powerful tool with which to transduce genes into target cells and tissues (Kaplitt *et al.*, 1994; Berns and Giraud, 1995; Xiao *et al.*, 1997; Schwarz, 2000), with several advantages over other virus vectors. The benefits include a lack of virulence in the wild type, an inherent inability to replicate itself, an ability to transduce nondividing cells and to integrate into a host genome, and long-term expression of the transduced gene. Furthermore, Goater *et al.* (2000) have shown there is a substantial integration rate of AAV into synovial tissue, but there has not been any quantitative analysis so far. Synovial tissue is the most abundant tissue in an articular joint, which makes it a formidable host for viral transfection.

From the advantages demonstrated by AAV, there would appear to be a distinct possibility that cartilage repair could be accomplished by transduction of the bFGF gene using AAV as a viral vector, and we hypothesizd that if the high level of integration into chondrocytes, as shown by Yokoo *et al.* (2005), could also be achieved in synoviocytes via intraarticular administration of AAV-bGFG, cartilage regeneration may result.

Therefore, in this study, we set out to evaluate the potency of the AAV vector, and to investigate whether articular cartilage repair is possible. Two methods were proposed: first, *in vitro*, to observe the efficiency of AAV as a gene transporter when targeted at synoviocytes, and second, *in vivo*, to determine whether cartilage regeneration is possible by intraarticular administration of AAV-bFGF into rabbit knee joints with chondral defects.

PILOT STUDIES

In vivo studies by Goater *et al.* (2000) confirmed high induction rates of AAV in synovial tissues. Our previous *ex vivo* studies (Kobayashi *et al.*, 2002; Yokoo *et al.*, 2005) also demonstrated that gene transduction was effective in both synoviocytes and chondrocytes. To reconfirm and establish our method protocol for the main experiments, a series of preliminary studies, in which AAV-LacZ was administered into synovial tissues of both knee joints of two rabbits, was performed. Subsequent 5-bromo-4-chloro-3-indolyl-β-D-galactopyranoside (X-Gal) staining confirmed both macroscopically and histologically, that gene tranduction was indeed effective and that a substantial transduction rate could be expected when synoviocytes were targeted by AAV. In another series, the optimal viral concentration was also determined by administering AAV-LacZ at various concentrations. The minimal dose was 1×10^5 particles, and the transfection rate was optimized at 1×10^9 particles (100 μl of solution containing 1×10^{10} particles/ml), after which the visible percentage of LacZ-positive cells reached a plateau. However, because of the inherent nature of a single synovium, we were unable to perform a precise quantitative analysis of LacZ-positive synoviocytes (details of the data obtained are not shown).

MATERIALS AND METHODS

AAV vector production

Two different adeno-associated viral constructs were prepared for the study: AAV-LacZ, carrying the bacterial β-galactosidase gene, a marker gene that can be detected by X-Gal staining; and AAV-bFGF, carrying the bFGF gene, which harbors a nuclear localization signal, under the regulation of the cytomegalovirus (CMV) immediate-early promoter. The AAV subtype 2 vector plasmid used was derived from the vector plasmid pW1 (hereafter referred to as pLacZ), which carries the *lacZ* gene (Price *et al.*, 1987). Recombinant bFGF gene was obtained from Takeda Pharmaceutical (Osaka, Japan; GenBank accession number X07285). A fragment containing bFGF cDNA was amplified by polymerase chain reaction (PCR) using the following primer pairs (*Eco*RI and *Xho*I sites are underlined): 5′-ATGAATTCATGGCTGCCGGCAGCATCACTTCGCTT-3′ and 5′-ATCTCGAGAGAGTCAGCTCTTAGCAGAC-3′. The fragment was subcloned between the *Eco*RI and *Xho*I sites of the pLacZ AAV vector plasmid to replace the *lacZ* gene (pbFGF). pIM45 is an AAV helper plasmid carrying subtype 2 AAV *rep* and *cap* genes, which are required for replication and caspid formation of AAV vectors. pladeno-1, a plasmid containing the E2A, E4, and VA genes of the adenovirus genome, was used in place of helper adenovirus for AAV production.

Subconfluent human fetal kidney cells (293 cells) were cotransfected by the calcium phosphate coprecipitation method

with pbFGF, pIM45, and pladeno-1 to produce the AAV inducing bFGF gene (AAV-bFGF). After 48 hr, cells were harvested and lysed in Tris-HCl buffer (10 m*M* Tris-HCl, 150 m*M* NaCl, pH 8.0) through three cycles of freezing and thawing. One round of sucrose precipitation and two rounds of CsCl density gradient ultracentrifugation were performed to isolate AAV-bFGF from the lysates. The vector titer was determined by quantitative DNA dot-blot hybridization of the DNase I-resistant fraction.

In vitro *study: examination of the potency of AAV as a viral vector when targeted at synoviocytes*

Isolation of synoviocytes. Five Japanese white rabbits (Oriental Yeast, Tokyo, Japan), 12 weeks old, weighing an average of 2.1 kg, were used for the study. Under intravenous anesthesia with pentobarbital sodium (Somnopentyl; Schering-Plough Animal Health, Union, NJ), synovial tissues were harvested from the knee joint, washed three times in phosphate-buffered saline (PBS), and cut into small pieces. These pieces were then treated with 0.25% collagenase (type II collagenase; Worthington Biochemical, Lakewood, NJ) for 2 hr at 37°C. The treated synoviocytes were washed three times with PBS and centrifuged for 5 min at 1500 rpm, and then equally divided into four separate flat-bottomed plates (Falcon [diameter, 30 mm]; BD Biosciences Discovery Labware, Bedford, MA) at 1×10^5 cells per plate in 1.0 ml of Dulbecco's modified Eagle's medium (DMEM; Sigma, St. Louis, MO) supplemented with 10% fetal calf serum (FCS) and antibiotics (penicillin G [100 U/ml] and streptomycin [0.1 mg/ml]; GIBCO-BRL Invitrogen, Carlsbad, CA) (DMEM–FCS), at 37°C in a 5% CO_2–air atmosphere for 48 hr.

Gene transduction into synoviocytes. After 48 hr in growth medium, the synoviocyte cultures were removed and washed once with serum-free DMEM. A 500-μl volume of serum-free DMEM containing AAV-LacZ was added to the control group culture plate, and 500 μl of serum-free DMEM containing AAV-bFGF was added to the gene-transduced group culture plate. This was to enable quantification of transgene expression at the optimal number of viral particles (10^7 particles per cell) determined from pilot studies (data not shown).

Five samples from the bFGF-transduced group and five from the control group (*lacZ*-transduced group) were used for the experiment to determine the efficiency of gene transduction *in vitro*. Culture medium was not exchanged during the examination period of 2 weeks. 3, 7, and 14 days after transduction, supernatant was removed, and LacZ expression in the LacZ group was assessed by the X-Gal staining technique (Yokoo *et al.*, 2005). The efficiency of gene transduction was calculated as the average percentage of X-Gal-positive cells per total living cells, determined by viewing three randomly selected fields (magnification, ×100) with an optical microscope.

Measurement of bFGF concentration in culture medium. Five samples from the bFGF-transduced group and five from the control group (*lacZ*-transduced group) were used to determine the accumulation of bFGF in culture supernatant. The culture medium of bFGF-transduced or control chondrocytes was not exchanged at each sampling. 3, 7, and 14 days after transduction, culture supernatants were collected from all four bFGF-transduced or control group culture wells and, after centrifugation, were stored at −80°C until analysis. The bFGF concentration in culture supernatants of both groups were measured by enzyme-linked immunosorbent assay (ELISA), using a bFGF-specific ELISA kit (Quantikine; R&D Systems, Minneapolis, MN) according to the manufacturer's instructions.

In vivo *study: cartilage regeneration by intraarticular administration of AAV-bFGF*

Intraarticular administration of AAV-bFGF into articular cartilage defect. Surgery and postoperative management were carried out under certification of the Yokohama City University Animal Center (Yokohama City, Japan) and with the approval of the Animal Care Committee.

Twenty-four Japanese white rabbits were used for the *in vivo* study. They were anesthetized as required by intravenous injection of pentobarbital sodium, and both knees were sterilized for surgery. A 2.5-cm medial parapatellar incision was made and the patella was dislocated laterally. A full-thickness defect (diameter, 5 mm; depth, 3 mm) was artificially created in the patellar groove of the anterior surface of the distal femur, using a hand drill bit; 1×10^9 particles (100 μl of solution containing 1×10^{10} particles/ml) of AAV-bFGF, which had been shown to be the optimal amount in our pilot study, was administered with a microsyringe, and the dislocated patella was reduced to its original position immediately. The same procedure was repeated for the contralateral knee. In the control group, the same procedure was followed, but 100 μl of phosphate-buffered saline (PBS) solution was administered instead of AAV-bFGF. The rabbits were allowed freedom of movement immediately after surgery. Four rabbits from each group were subsequently killed at 4, 8, and 12 weeks for macroscopic and histological examination of the articular surface of both knees.

Macroscopic and histological evaluation of repaired cartilage. To enable comparative examination of the articular components, four animals (both knees) from the AAV-bFGF group, and an equivalent number from the PBS (control) group, were sacrificed at 4, 8, and 12 weeks. Macroscopic assessment and photography were followed by *en bloc* resection of the distal end of the femur. The specimens were fixed with 10% buffered formaldehyde for 1 week, followed by decalcification with 0.5 *M* EDTA solution for 2 to 3 weeks. Sagittal sections through cartilaginous tissue and bone were prepared and stained with hematoxylin and eosin (H&E) and safranin O. Macroscopic findings for each specimen were evaluated semiquantitively according to the scale described by Kumagai *et al.* (2003). The Kumagai Scale for Macroscopic Assessment of Cartilage Surface is an established system of parameters for grading specimens in color (0–3), connection of new tissue to adjacent cartilage (0–2), size of remaining defect (0–5), depression of the defect (0–4), and depth of the defect (0–2). The overall score scales from zero, suggesting full repair, to 16, indicating no repair.

Likewise, histological findings for each specimen were evaluated semiquantitatively according to the scale described by Wakitani *et al.* (1994). The Wakitani Scale for Histological As-

sessment of Cartilage Defects is an established system of parameters for grading specimens in cell morphology (0–4), matrix staining (0–3), surface regularity (0–3), thickness of cartilage (0–2), and integration of donor with adjacent host cartilage (0–2). The overall score scales from zero, suggesting full repair, to 14, indicating no repair.

Evaluation of supernatant bFGF concentration after in vivo *study.* At the time of sacrifice, synovial tissue was harvested for examination of bFGF concentration after *in vivo* administration of AAV-bFGF. Harvested tissues were treated with 0.25% type II collagenase as previously described, and cultured for 1 week at 37°C without exchange of medium. Supernatant of the synoviocyte cultures from the bFGF group and from the control group were analyzed at 4, 8, and 12 weeks and evaluated by the ELISA method.

Immunohistological assessment for type II collagen in cell matrix. Immunohistological assessment targeted the type II collagen seen in the extracellular matrix of the regenerated cartilage, using rabbit anti-type II collagen antibody (Santa Cruz Biotechnology, Santa Cruz, CA).

Statistical analysis. Data were expressed as means ± standard deviation (SD). The statistical significance of differences was calculated with StatView version J-5.0 (SAS Institute, Cary, NC). One-way analysis of variance (ANOVA) and the Mann–Whitney *U* test were used for analyzing statistical significance. *p* Values less than 0.05 were considered significant.

RESULTS

In vitro *study: examination of the potency of AAV as a viral vector when targeted at synoviocytes*

Efficiency of gene transduction into synoviocytes: LacZ expression. Values for synoviocytes transfected with AAV-LacZ were determined at intervals of 3, 7, and 14 days after transduction. The percentage of LacZ-positive cells among total living cells was determined to be 55.8 ± 6.0 (mean ± SD), 83.4 ± 3.8, and 92.0 ± 1.6%, respectively, at an optimal dose of 10^7 particles per cell (Table 1). The percentage of successfully transduced synoviocytes increased in a vector dose-dependent manner up to an optimal figure of 10^7 particles per cell, when approximately 100% efficiency was achieved. Doses of viral particles above that level failed to improve the transduction rate. Microscopic examination did not reveal any evidence of cell death or cytopathic change in the transduced cells.

bFGF gene expression in transduced synoviocytes. bFGF production was detected in both bFGF-transduced and control cells. bFGF concentration in the culture supernatant was 31.2 ± 7.8, 80.5 ± 16.4, and 120.8 ± 22.5 ng/ml at 3, 7, and 14 days after transduction, respectively, in bFGF-transduced cells (Table 1). In control cells, the bFGF concentration was 22.6 ± 9.2, 23.1 ± 6.4, and 28.4 ± 7.8 ng/ml at 3, 7, and 14 days after transduction, respectively. The bFGF concentration was significantly greater in bFGF-transduced cells than in control cells at each sampling time point ($p < 0.01$).

In vivo *study: cartilage regeneration by intraarticular administration of AAV-bFGF*

Macroscopic findings on cartilage regeneration. Observation of the articular cartilage defect site showed regeneration in both the bFGF-transduced and control groups. At 4 weeks, cartilage regeneration was not obvious in the control group (Fig. 1A), whereas partial coverage by regenerated cartilage was seen in the AAV-bFGF group (Fig. 1B). At 8 weeks, the difference in cartilage regeneration became more apparent (Fig. 1C and D) and at 12 weeks, the margin between the regenerated tissue and the original cartilage was not distinguishable in the AAV-bFGF group (Fig. 1F), whereas the margin was clearly visible in the control group (Fig. 1E).

Histological findings on cartilage regeneration. At 4 weeks after administration of AAV-bFGF, tissues obtained from the bFGF-transduced group showed slight formation of a chondral layer in the deep part of the cartilage defect. Tissue was composed of round chondrocytes with weakly safranin O-stained extracellular matrix (Fig. 2B). There was no integration of the edges of regenerated tissue with normal adjacent cartilage or reconstitution of the osteochondral junction in any specimen. In the control group, the extracellular matrix was hardly stained with safranin O (Fig. 2A), and no cartilage regeneration was

TABLE 1. TIME-DEPENDENT LacZ EXPRESSION AND SUPERNATANT bFGF CONCENTRATION IN CULTURED SYNOVIOCYTES[a]

Days after transfection	*Percentage of LacZ-positive cells*	*bFGF concentration (ng/ml)*	
		AAV-bFGF group[b]	*Control group*[b]
3	55.8 ± 6.0	31.2 ± 7.8	22.6 ± 9.2
7	83.4 ± 3.8	80.5 ± 16.4	23.1 ± 6.4
14	92.0 ± 1.6	120.8 ± 22.5	28.4 ± 7.8

[a]LacZ expression was assessed by X-Gal staining 3, 7, and 14 days after AAV-LacZ transduction of chondrocytes. Values represent mean percentages ± SD. bFGF concentration of the supernatant was analyzed by ELISA 3, 7, and 14 days after AAV-bFGF transduction of synoviocytes. Values represent mean concentrations (ng/ml) ± SD. $n = 5$.

[b]$p < 0.01$.

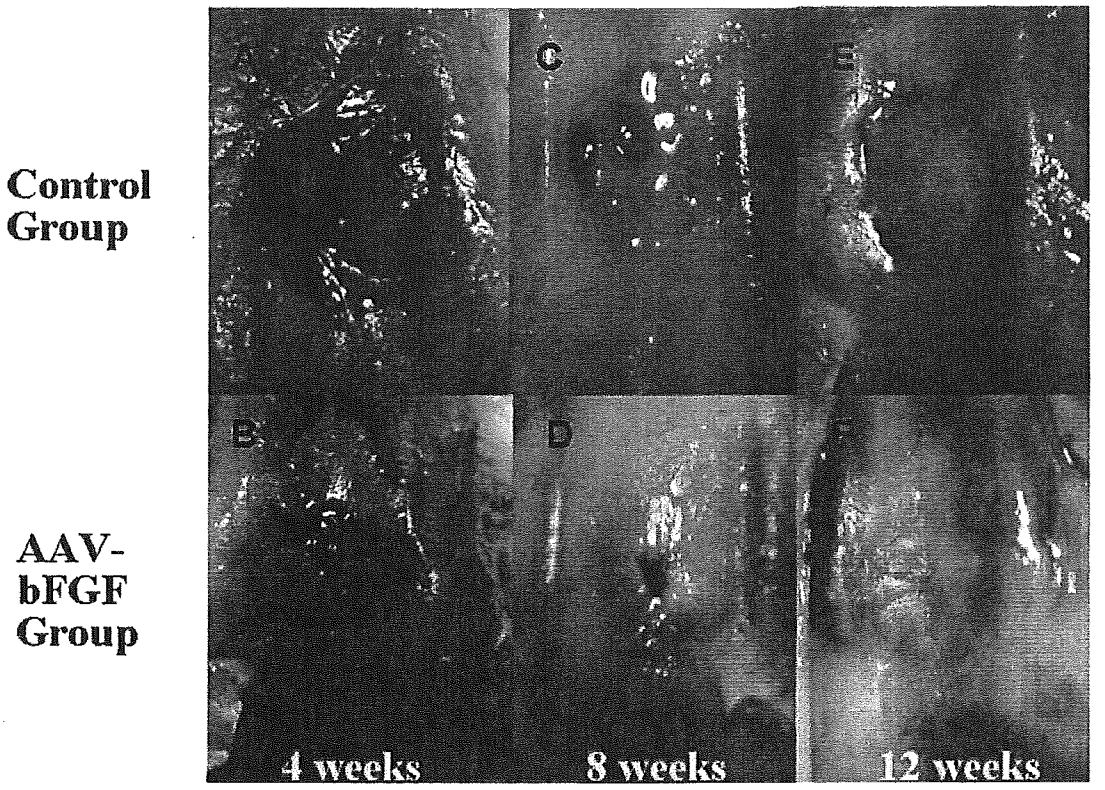

FIG. 1. Macroscopic photographs showing cartilage repair after interarticular administration of AAV-bFGF and control at 4, 8, and 12 weeks after operation. At 12 weeks in the AAV-bFGF group, almost complete repair is seen, whereas in the control group, the margin between the newly formed cartilage and the surrounding normal cartilage is obvious.

seen. The tissues showed inflammatory granulation of the defect area, and any bone may have been partly obscured because of apoptosis and replacement of fibrous tissues.

At 8 weeks, in the bFGF-transduced group, the extracellular matrix was more distinctly stained with safranin O, and cartilage regeneration was seen not only in the deep part, but also in the superficial layer (Fig. 2D). Both edges of the regenerated cartilage showed almost complete integration with normal adjacent cartilage, and reconstitution of the osteochondral junction was seen in five specimens. In Fig. 2C, tissues from the control group were essentially the same as those seen at 4 weeks. Although safranin O staining appears stronger, there is no apparent formation of hyaline cartilage and no construct of mature cartilage tissue is visible.

In the bFGF-transduced group at 12 weeks, the intensity and thickness of the extracellular matrix were increased when compared with the findings at 4 and 8 weeks, and the microstructure of the regenerated tissue resembled the surrounding normal cartilage (Fig. 2F). There was reconstitution of the osteochondral junction in most specimens, and formation of the surface layer of articular cartilage was distinctly more pronounced in contrast to that shown in the control (Fig. 2E). In the control group, formation of hyaline cartilage-like tissue was seen in three specimens, but others presented formation of fibrous cartilage. Extracellular matrix stained well with safranin O in three specimens, but was less compared with the bFGF group. There was no reconstitution of the osteochondral junction in any specimen.

Semiquantitive macroscopic and histological analyses. Semiquantitive analysis using the Kumagai Scale showed a significant difference in the two groups ($p < 0.01$) as detailed in Table 2. At 4, 8, and 12 weeks, average macroscopic scores in the AAV-bFGF group were 9.25 ± 2.21, 2.25 ± 0.70, and 0.25 ± 0.12 points, and the surface of the regenerated cartilage closely resembled normal cartilage in the bFGF-transduced group. On the other hand, macroscopic scores in the control group showed an average of 12.0 ± 2.34, 8.50 ± 1.72, and 5.00 ± 1.28 points at 4, 8, and 12 weeks, respectively, and regenerated cartilage could still be distinguished from surrounding normal cartilage even at 12 weeks. No sign of osteoarthrosis, such as erosion of cartilage or formation of osteophytes, was recognized in any of the joint surfaces during the observation period. Tumor formation was also not recognized, but there was a slight hyperplastic change in the lateral condyle in one knee joint of the bFGF group. No hyperplasia of synovium was seen in any of the joints of the bFGF-transduced group.

Histological analysis using the Wakitani score showed 6.75 ± 1.15, 2.25 ± 0.67, and 0.75 ± 0.33 points at 4, 8, and 12 weeks after AAV-bFGF administration, respectively (Table 2). In the control group, the score was 13.5 ± 1.0, 11.0 ± 1.5, and 5.00 ± 2.00 points at 4, 8, and 12 weeks respectively. The scores in both groups decreased throughout the experimental period. However, the score in the bFGF-transduced group became significantly lower than that in the control group over time ($p < 0.01$).

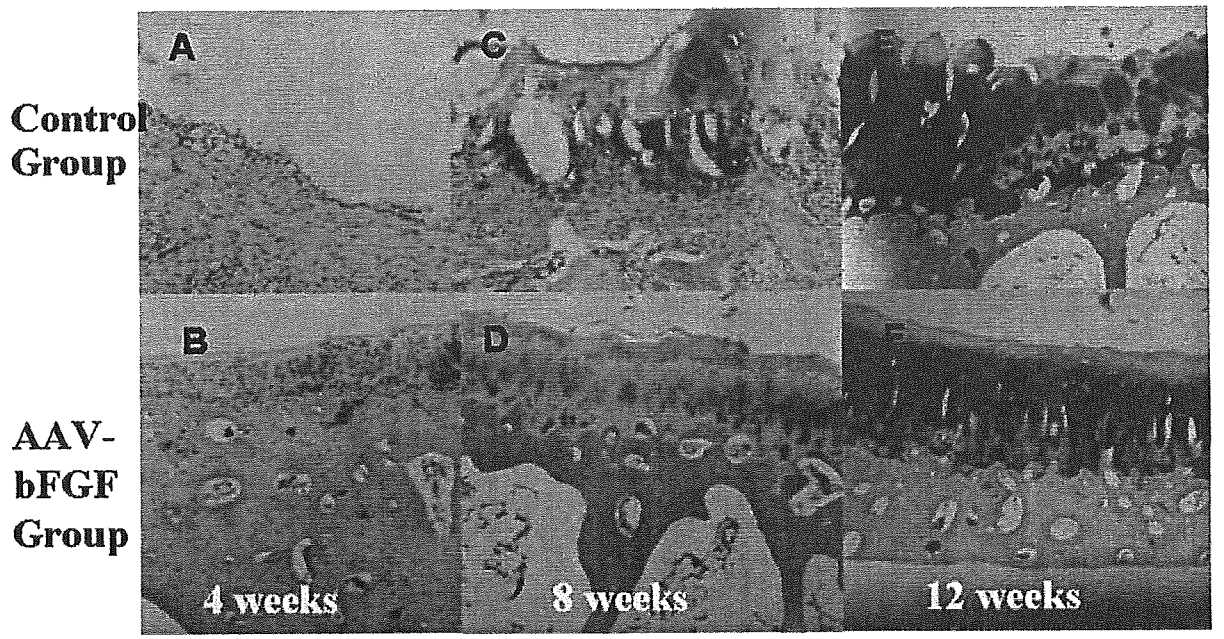

FIG. 2. Histological assessment of prepared sagittal sections using safranin O and hematoxylin staining. At 4 weeks (**A**) control group extracellular matrix is hardly stained, no cartilage regeneration is seen, but the tissues show inflammatory granulation of the defect area, which may obscure any bone because of apoptosis and replacement of fibrous tissue. (**B**) bFGF-transduced group matrix is lightly stained and the deep part is composed of rounded chondrocytes. At 8 weeks (**C**) partial chondrocyte repair is seen, with limited metachromasy. (**D**) The matrix is more distinctly stained and cartilage regeneration has advanced to the superficial layer. At 12 weeks (**E**) generation of chondrocyte-like cells with irregular matrix formation is seen, but no reconstitution of the bone–cartilage junction is apparent. (**F**) Note the intensely stained matrix, reconstitution of the osteochondral junction, and formation of the surface layer of the articular cartilage.

bFGF concentration in synovial cell culture after in vivo *administration of AAV-bFGF.* bFGF production was detected in both bFGF-transduced and control cells. bFGF concentration in the culture supernatant was 133.8 ± 15.6, 122.5 ± 19.3, and 94.0 ± 8.4 ng/ml at 4, 8, and 12 weeks after transduction, respectively, in bFGF-transduced cells (Fig. 3). In control cells, bFGF concentration was 34.0 ± 7.8, 19.5 ± 6.3, and 21.0 ± 2.7 ng/ml at 4, 8, and 12 weeks after transduction, respectively. bFGF concentration was significantly greater in bFGF -transduced cells than in control cells on all days of sampling ($p < 0.01$).

Immunohistological assessment of the cell matrix. Immunohistological assessment of the extracellular matrix was made in the AAV-bFGF group at 8 and 12 weeks. The antibody was targeted at extracellular matrix, and clear staining was seen at both 8 and 12 weeks, when compared with the control group (Fig. 4).

DISCUSSION

Because of its limited self-repairing nature, regeneration of cartilage is a difficult task, and clinical attempts have been made

TABLE 2. SEMIQUANTITIVE MACROSCOPIC AND HISTOLOGICAL ANALYSIS OF bFGF-TRANSDUCED CARTILAGE[a]

Weeks after transduction	*Macroscopic score*[b]		*Histological score*[b]	
	AAV-bFGF-F	*Control*	*AAV-bFGF*	*Control*
4	9.25 ± 2.21	12.0 ± 2.34	6.75 ± 1.15	13.5 ± 1.00
8	2.25 ± 0.70	8.50 ± 1.72	2.25 ± 0.67	11.0 ± 1.50
12	0.25 ± 0.12	5.00 ± 1.28	0.75 ± 0.33	5.00 ± 2.00

[a]Semiquantitive macroscopic and histological scores comparing the AAV-bFGF group and control group at 4, 8, and 12 weeks after administration. Macroscopic scoring system: 0 points, maximum with complete repair; 16 points, minimum with no repair. Histological scoring system: maximum and minimum scores are 0 and 14 points, respectively. $n = 8$.

[b]$p < 0.01$.

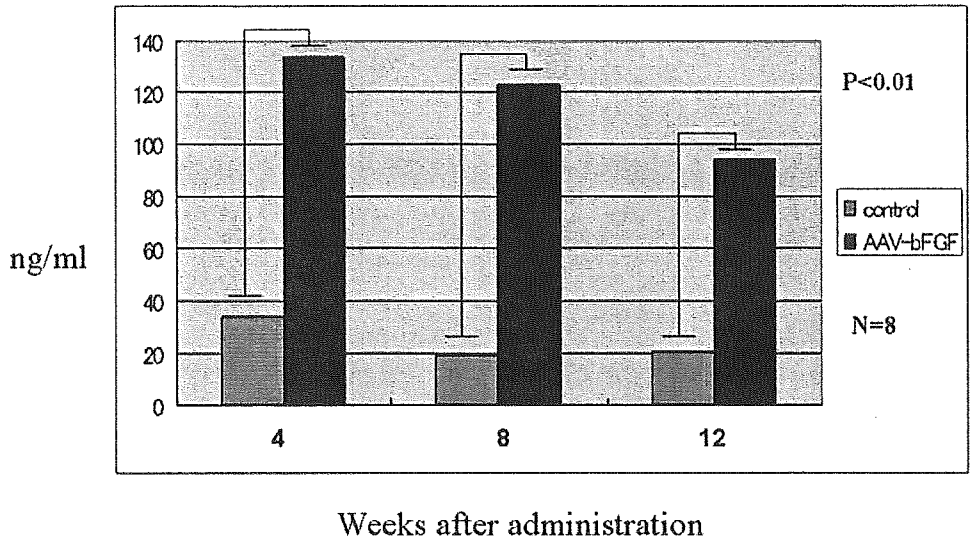

FIG. 3. bFGF concentration in culture supernatant of bFGF-transduced synoviocytes 4, 8, and 12 weeks after AAV-bFGF administration. Culture supernatants of control and bFGF-transduced cells were collected 7 days after harvesting and culture, and bFGF concentration was determined by ELISA. Transduction of the bFGF gene significantly elevates the secretion of bFGF ($*p < 0.01$).

to repair human cartilage, such as implantation of autologous chondrocytes (Richardson *et al.*, 1999), which have proven successful. In these cases, autologous chondrocyte grafts, harvested from non-weight-bearing areas, were cultured *in vitro* and then reinserted into the cartilage defect with coverage by a periosteal flap. However, because of the limited amount of graft tissue that can be obtained from the donor site, the method is limited to small local cartilage defects. Another successful method used clinically is mosaicplasty, used in diseases such as osteochondritis dissecans, but again, patients are limited to those who suffer only from small local cartilage defects. Given these limitations, a more fundamental method for cartilage repair would seem to be needed.

With numerous studies concerning growth factors, and discovery of potent gene transporters, methods to transport these genes into target organs have come to light (Kaplitt *et al.*, 1994; Berns and Giraud, 1995; Xiao *et al.*, 1997; Schwarz, 2000). Thus, gene therapy has become one of the most powerful tools for treatment of degenerative disorders, but still has several problems: the first, and perhaps most important, is that of safety—that is, in terms of virus virulence and their ability to self-reproduce; the second concerns their capacity to integrate into the host genome; and the third is the issue of long-term gene expression.

Adeno-associated virus (AAV), which was first discovered in research of its hosting virus, the adenovirus, has several bi-

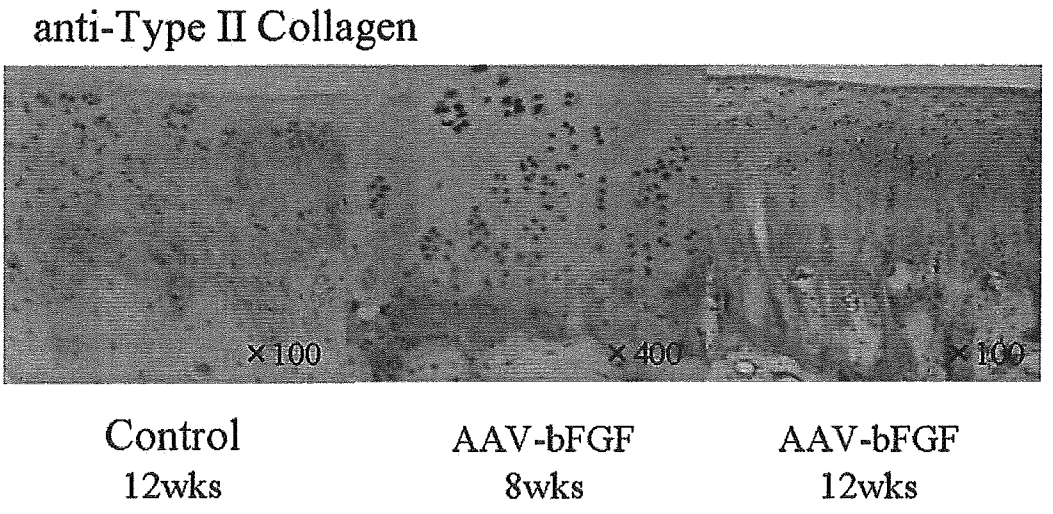

FIG. 4. Immunohistological staining for type II collagen. Staining is not seen in the negative control at 12 weeks. Staining of the extracellular matrix is seen at 8 weeks, and is most strong 12 weeks after AAV-bFGF administration.

ological advantages over other viral gene transporters, and the only apparent disadvantage is its small size, which may limit the size of the gene it can carry. It is most important to obtain high-efficiency transduction and continuous local expression of the therapeutic gene for repair of cartilage defects by gene therapy. Several studies have demonstrated the high ability of the AAV as a gene transporter, and its ability to express the transduced gene for a certain length of time (Kessler *et al.*, 1996; Fisher *et al.*, 1997; Herzog *et al.*, 1997). There are also reports of the utility of the AAV vector in the treatment of joint diseases, in which it demonstrated high-efficiency gene delivery into the synovium *in vivo* (Goater *et al.*, 2000), and gene transduction into cultured chondrocytes *in vitro* (Arai *et al.*, 2000). In our previous study, *ex vivo* gene transfer to periosteum-derived cells, using an AAV vector, induced *lacZ* gene expression for 4 weeks *in vivo* (Kobayashi *et al.*, 2002). However, the *ex vivo* method is complex, and may not be practical in terms of clinical therapy. On the other hand, delivering genes directly to the surface of abnormal articular cartilage could result in long-term treatment to accelerate cartilage repair.

Augmentation of cartilage repair by application of basic fibroblast growth factor (bFGF) has been reported to be efficient (Shida *et al.*, 1996; Cuevas *et al.*, 1988). Weisser *et al.* (2001) documented that by transplanting chondrocytes treated with several growth factors, positive effects on cartilage repair were observed only in bFGF-treated chondrocyte implants, and Fujimoto *et al.* (1999) showed that *in situ* delivery of bFGF also enhanced the ability to repair cartilage. Other studies have also shown that exogenous bFGF induced proliferation of chondrocytes, maturation of cartilage, and differentiation of mesenchymal cells, and stimulated synthesis of cartilaginous matrix (Cuevas *et al.*, 1988; Shida *et al.*, 1996). Otsuka *et al.* (1997) described how continuous administration of bFGF, using an osmotic pump, had a clear beneficial effect on repair of cartilage defects.

After considering the above-described findings, we were led to believe that achieving integration of the bFGF gene into intraarticular tissues, such as synoviocytes, by intraarticular administration could result in long-term expression and prolonged secretion of the growth factor, and culminate in regeneration of cartilage.

In this study, high-efficiency *lacZ* gene transduction to synoviocytes was obtained *in vitro*, and bFGF gene expression was detected in both bFGF-transduced and control cells. Subsequently, gene expression *in vivo* was sustained for at least 12 weeks without any adverse effects, and the findings suggest that *in vivo* gene transfer to articular cartilage defects, using the AAV vector, was successful.

We have shown that bFGF secretion was significantly increased in bFGF-transduced synoviocytes compared with the control groups, both *in vitro* and *in vivo*. Furthermore, repair at a relatively early stage was noticeably different between the bFGF-transduced and control cartilage tissue, and the eventual histological appearance of the transfected site in the bFGF-transduced group showed full repair compared with the control group, where the difference was still visible.

The results demonstrate that repair of full-thickness defects in rabbit articular cartilage can be enhanced by intraarticular administration of AAV-bFGF, by a procedure that is much less complex compared with the orthodox *ex vivo* method, and that is equally, if not more, effective.

Hence, it can be concluded that continuous bFGF secretion by gene transfer was extremely effective in promoting cartilage repair, demonstrating that this approach could in future be used clinically as a potent method for repair of cartilaginous diseases. However, further long-term studies will be necessary to assess the final outcome of regenerated articular cartilage.

ACKNOWLEDGMENTS

Supported in part by grants from the Grant-in-Aid for Scientific Research from the Ministry of Education, Culture, Sports, Science, and Technology of Japan.

REFERENCES

ARAI, Y., KUBO, T., KOBAYASHI, K., TAKESHITA, K., TAKAHASHI, K., IKEDA, T., IMANISHI, J., TAKIGAWA, M., and HIRASAWA, Y. (1997). Adenovirus vector-mediated gene transduction to chondrocytes: *In vitro* evaluation of therapeutic efficiency of transforming growth factor-β_1 and heat shock protein 70 gene transduction. J. Rheumatol. **24,** 1787–1795.

ARAI, Y., KUBO, T., FUSHIKI, S., MAZDA, O., NAKAI, H., IWAKI, Y., IMANISHI, J., and HIRASAWA, Y. (2000). Gene delivery to human chondrocytes by an adeno-associated virus vector. J. Rheumatol. **27,** 979–982.

BARAGI, V.M., RENKIEWICZ, R.R., QIU, L., BRAMMER, D., RILEY, J.M., SIGLER, R.E., FRENKEL, S.R., AMIN, A., ABRAMSON, S.B., and ROESSLER, B.J. (1997). Transplantation of adenovirally transduced allogenic chondrocytes into articular cartilage defects *in vivo*. Osteoarthritis Cartilage **5,** 275–282.

BERNS, K.I., and GIRAUD, C. (1995). Adenovirus and adeno-associated virus as vectors for gene therapy. Ann. N.Y. Acad. Sci. **772,** 95–104.

BRITTBERG, M., LINDAHL, A., NILSSON, A., OHLSSON, C., ISAKSSON, O., and PETERSON, L. (1994). Treatment of deep cartilage defects in the knee with autologous chondrocyte transplantation. N. Engl. J. Med. **331,** 889–895.

CUEVAS, P., BURGOS, J., and BAIRD, A. (1988). Basic fibroblast growth factor (FGF) promotes cartilage repair *in vivo*. Biochem. Biophys. Res. Commun. **156,** 611–618.

DOHERTY, P.J., ZHANG, H., TREMBLAY, L., MANOLOPOULOS, V., and MARSHALL, K.W. (1998). Resurfacing of articular cartilage explants with genetically modified human chondrocytes *in vitro*. Osteoarthritis Cartilage **6,** 153–159.

FISHER, K.J., JOOSS, K., ALSTON, J., YANG, Y., HAECKER, S.E., HIGH, K., PATHAK, R., RAPER, S.E., and WILSON, J.M. (1997). Recombinant adeno-associated virus for muscle directed gene therapy. Nat. Med. **3,** 306–312.

FUJIMOTO, E., OCHI, M., KATO, Y., MOCHIZUKI, Y., SUMEN, Y., and IKUTA, Y. (1999). Beneficial effect of basic fibroblast growth factor on the repair of full-thickness defects in rabbit articular cartilage. Arch. Orthop. Trauma Surg. **119,** 139–145.

GOATER, J., MULLER, R., KOLLIAS, G., FIRESTEIN, G.S., SANZ, I., O'KEEFE, R.J., and SCHWARZ, E.M. (2000). Empirical advantages of adeno associated viral vectors for *in vivo* gene therapy for arthritis. J. Rheumatol. **27,** 983–989.

HERZOG, R.W., HAGSTROM, J.N., KUNG, S.H., TAI, S.J., WILSON, J.M., FISHER, K.J., and HIGH, K.A. (1997). Stable gene transfer and expression of human blood coagulation factor IX after intramuscular injection of recombinant adeno-associated virus. Proc. Natl. Acad. Sci. U.S.A. **94,** 5804–5809.

HUNZIKER, E.B., and ROSENGERG, L.C. (1996). Repair of partial-thickness defects in articular cartilage: Cell recruitment from the synovial membrane. J. Bone Joint Surg. Am. **78,** 721–733.

KANG, R., MARUI, T., GHIVIZZANI, S.C., NITA, I.M., GEORGESCU, H.I., SUH, J.K., ROBBINS, P.D., and EVANS, C.H. (1997). *Ex vivo* gene transfer to chondrocytes in full-thickness articular cartilage defects: A feasibility study. Osteoarthritis Cartilage **5,** 139–143.

KAPLITT, M.G., LEONE, P., SAMULSKI, R.J., XIAO, X., PFAFF, D.W., O'MALLEY, K.L., and DURING, M.J. (1994). Long-term gene expression and phenotypic correction using adeno-associated virus vectors in the mammalian brain. Nat. Genet. **8,** 148–154.

KESSLER, P.D., PODSAKOFF, G.M., CHEN, X., MCQUISTON, S.A., COLOSI, P.C., MATELIS, L.A., KURTZMAN, G.J., and BYRNE, B.J. (1996). Gene delivery to skeletal muscle results in sustained expression and systemic delivery of a therapeutic protain. Proc. Natl. Acad. Sci. U.S.A. **93,** 14082–14087.

KOBAYASHI, N., KOSHINO, T., UESUGI, M., YOKOO, N., XIN, K.Q., OKUDA, K., MIZUKAMI, H., OZAWA, K., and SAITO, T. (2002). Gene marking in adeno-associated virus vector infected periosteum-derived cells for cartilage repair. J. Rheumatol. **29,** 2176–2180.

KUMAGAI, K., SAITO, T., and KOSHINO, T. (2003). Articular cartilage repair of rabbit chondral defect promoted by creation of periarticular bony defect. J. Orthop. Sci. **8,** 700–706.

OTSUKA, Y., MIZUTA, H., TAKAGI, K., IYAMA, K., YOSHITAKE, Y., NISHIKAWA, K., SUZUKI, F., and HIRAKI, Y. (1997). Requirement of fibroblast growth factor signaling for regeneration of epiphyseal morphology in rabbit full-thickness defects of articular cartilage. Dev. Growth Differ. **39,** 143–156.

PRICE, J., TURNER, D., and CEPKO, C. (1987). Lineage analysis in the vertebrate nervous system by retrovirus-mediated gene transfer. Proc. Natl. Acad. Sci. U.S.A. **84,** 156–160.

RICHARDSON, J.B., CATERSON, B., EVANS, E.H., ASHTON, B.A., and ROBERTS, S. (1999). Repair of human articular cartilage after implantation of autologous chondrocytes. J. Bone Joint Surg. Br. **81,** 1064–1068.

SCHWARZ, E.M. (2000). The adeno-associated virus vector for orthopaedic gene therapy. Clin. Orthop. **379S,** 31–39.

SHIDA, J., JINGUSHI, S., IZUMI, T., IWAKI, A., and SUGIOKA, Y. (1996). Basic fibroblast growth factor stimulates articular cartilage enlargement in young rats *in vivo*. J. Orthop. Res. **14,** 265–272.

WAKITANI, S., GOTO, T., PINEDA, S.J., YOUNG, R.G., MANSOUR, J.M., CAPLAN, A.I., and GOLDBERG, V.M. (1994). Mesenchymal cell-based repair of large, full-thickness defects of articular cartilage. J. Bone Joint Surg. Am. **76,** 579–592.

WEISSER, J., RAHFOTH, B., TIMMERMANN, A., AIGNER, T., BRAUER, R., and VON DER MARK, K. (2001). Role of growth factors in rabbit articular cartilage repair by chondrocytes in agarose. Osteoarthritis Cartilage **9**(Suppl. A), S48–S54.

XIAO, X., LI, J., MCCOWN, T.J., and SAMULSKI, R.J. (1997). Gene transfer by adeno-associated virus vectors into the central nervous system. Exp. Neurol. **144,** 113–124.

YOKOO, N., SAITO, T., UESUGI, M., KOBAYASHI, N., XIN, K.Q., OKUDA, K., MIZUKAMI, H., OZAWA, K., and KOSHINO, T. (2005). Repair of articular cartilage defect by autologous transplantation of basic fibroblast growth factor gene-transduced chondrocytes with adeno-associated virus vector. Arthritis Rheum. **52,** 164–170.

Address reprint requests to:
Dr. Atsuo Hiraide
Department of Orthopedic Surgery
Yokohama City University School of Medicine
3-9 Fukuura, Kanazawa-ku
Yokohama 236-0004, Japan

E-mail: arzt2001@h9.dion.ne.jp

Received for publication August 3, 2005; accepted after revision October 12, 2005.

Published online: November 4, 2005.